iScience

CellPress
OPEN ACCESS

Article

Resolving transitions between distinct phases of memory consolidation at high resolution in *Caenorhabditis elegans*

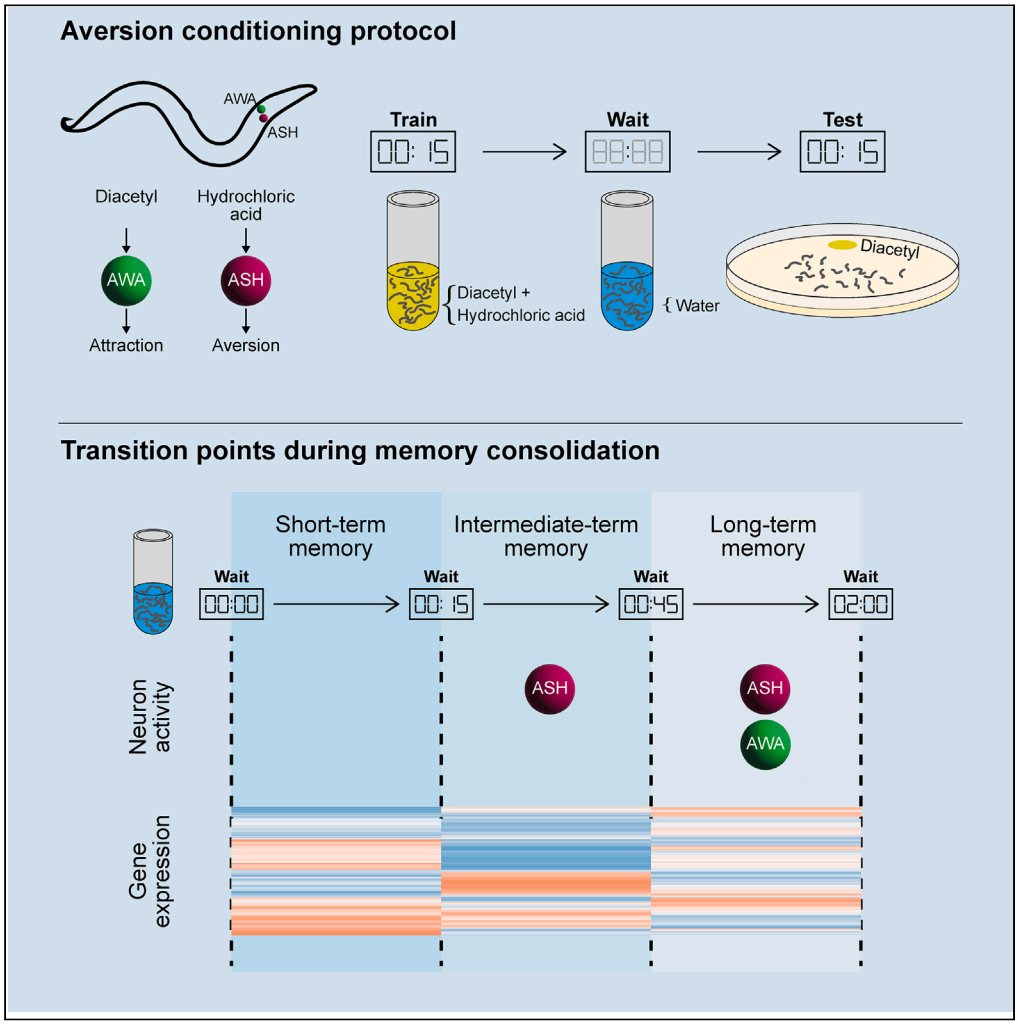

Netanel Cohen,
Ithai Rabinowitch

ithai.rabinowitch@mail.huji.ac.il

Highlights

Developed rapid, efficient, and robust *C. elegans* aversive learning protocol

Memory transitions are highly regulated, beginning immediately after learning

Sensory neurons play critical roles during memory consolidation

Coordinated gene transcription waves regulate short and long-term memory retention

Cohen & Rabinowitch, iScience *27*, 111147
November 15, 2024
https://doi.org/10.1016/j.isci.2024.111147

iScience

CellPress
OPEN ACCESS

Article

Resolving transitions between distinct phases of memory consolidation at high resolution in *Caenorhabditis elegans*

Netanel Cohen[1] and Ithai Rabinowitch[1,2,*]

SUMMARY

Memory consolidation following learning is a dynamic and complex process comprising several transitions between distinct memory phases. Although memory consolidation has been studied extensively, it remains difficult to draw an integral description that can delimit the transition points between specific memory phases at the behavioral, neuronal, and genetic levels. To this end, we have developed a rapid and robust aversive conditioning protocol for the nematode worm *Caenorhabditis elegans*, tracing memory consolidation within the first hour post conditioning and then up to 18 h post conditioning. This made it possible to uncover time-dependent involvement of primary sensory neurons, transcription and translation processes, and diverse gene populations in memory consolidation. The change in neuronal valence was strong enough to induce second order conditioning, and was amenable to considerable modulation in specific mutant strains. Together, our work lends memory consolidation to detailed temporal and spatial analysis, advancing system-wide understanding of learning and memory.

INTRODUCTION

Animals continuously adjust their behavior to subsist in a dynamic environment, where dangers and opportunities constantly arise.[1,2] This is achieved by multiple forms of behavioral plasticity, including associative learning, whereby the simultaneous occurrence of distinct conditioned and unconditioned stimuli (CS and US), leads to a change in the response to the CS.[3,4] The process of learning, memory formation, and memory consolidation comprise a sequence of steps,[5] including the acquisition of new information, transition between short-, intermediate-, and long-term memory,[6,7] and subsequently, forgetting.[8,9] The extent to which these steps are interdependent or rely on separate underlying processes is unclear.

Despite its relatively simple nervous system, the nematode worm *Caenorhabditis elegans*, like many other animals, can encode memory following associative learning, store the newly acquired memory for short term, and consolidate it to a more stable and long-lasting memory.[4,10,11] Past research on short-, intermediate-, and long-term memory in *C. elegans* following conditioning employed one of two conditioning schemes, often termed massed or spaced training.[12,13] Massed training consists of a single conditioning episode, generating both short- and intermediate-term memory, lasting minutes to hours. Spaced training comprises several conditioning episodes, and can induce long-term memory, persisting for at least 24 h.[12,13] Short-, intermediate-, and long-term memory can be differentiated using, for example, heat shock[14] or cold shock,[15] as well as by suppression of transcription or translation.[16,17] It is generally thought that short-term memory is independent of transcription or translation,[18] intermediate-term memory is dependent on translation but not transcription[7] and long-term memory is both transcription- and translation-dependent.[7,19]

We thus sought to examine these different memory phases and the transitions between them at the behavioral, neuronal, and genetic levels, following associative learning in *C. elegans*. To this end, we developed a simple aversive conditioning procedure, consisting of a single 15-min treatment with an attractive CS odor, diacetyl (DA), and noxious US, hydrochloric acid (HCl). The choice of a specific noxious stimulus[13] as a US rather than an overall adverse state, such as starvation or pathogenic bacteria,[20] was intended to restrict as much as possible the response to the US to particular neurons, as opposed to a systemic reaction often elicited during aversive conditioning. Such brief coupling of DA and HCl robustly produced memory lasting at least 4 h, making it possible to probe the transition between distinguishable memory phases, and to study patterns of neuronal, transcriptional and translational epochs during this process.

[1]Department of Medical Neurobiology, Institute for Medical Research Israel-Canada, Faculty of Medicine, Hebrew University of Jerusalem, Jerusalem 9112002, Israel
[2]Lead contact
*Correspondence: ithai.rabinowitch@mail.huji.ac.il
https://doi.org/10.1016/j.isci.2024.111147

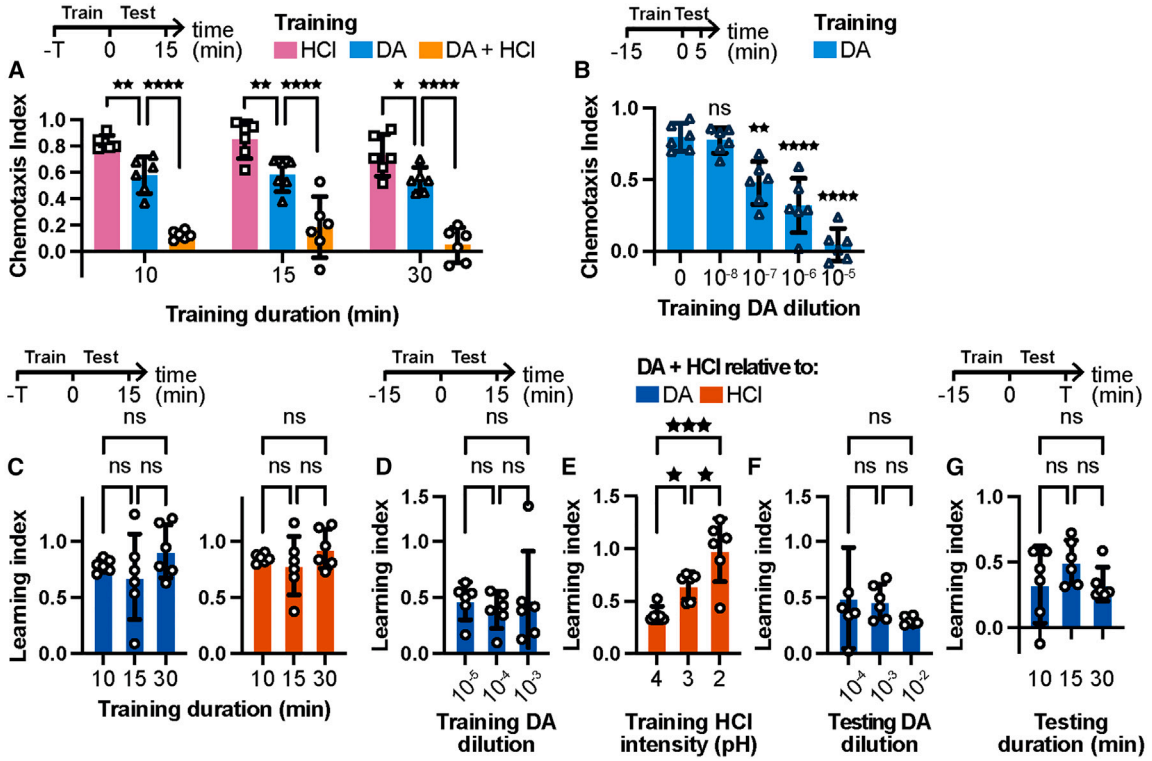

Figure 1. Aversive conditioning of the attractive odorant diacetyl (DA) to hydrochloric acid (HCl)

(A) Aversive conditioning induced by T = 10,15,30 min immersion of naive worms in a solution containing DA and HCl, followed by DA chemotaxis testing, compared to control exposure to HCl alone or DA alone.

(B) Chemotaxis to DA after training with DA alone at variable dilutions (1:1,000 testing dilution and 5 min testing duration).

(C) The difference in chemotaxis between trained and control worms with varying training durations (T = 10,15, 30 min) (A) is used to derive a Learning index, relative to DA, left, or HCl, right.

(D and E) Learning index derived from chemotaxis to DA after 15 min training with variable DA dilutions (D) or HCl pH (E).

(F and G) Learning index for a range of testing DA dilutions (F) and durations (T = 10,15,30 min) (G). Error bars indicate mean ±95% confidence intervals. $^{\star}p < 0.05$, $^{\star\star}p < 0.01$, $^{\star\star\star}p < 0.001$, $^{\star\star\star\star}p < 0.0001$. Details of the statistical analyses can be found in Data S1. Details of experimental parameters can be found in Table S2.

RESULTS

Brief exposure to attractant and repellant induces robust aversive conditioning

To gain new understanding of the temporal dynamics and the processes underlying memory consolidation following associative learning, we sought to develop an experimental paradigm for inducing rapid, specific, and robust aversive conditioning in *C. elegans*. Aversive conditioning occurs when an animal encounters an attractive conditioned stimulus (CS) together with a repulsive unconditioned stimulus (US), leading to reduced attraction to the CS. Brief training with HCl (US) and DA (CS), considerably decreased chemotaxis to DA compared to exposure to HCl or DA alone (Figure 1A).

In parallel to the conditioned response, we observed also a smaller non-associative reduction in DA attraction following exposure to DA alone, due to adaptation (Figure 1A, DA alone compared to HCl alone). The effect of adaptation was dilution-dependent (Figure 1B), detectable for a broad range of DA training and testing conditions (Figures S1A and S1B), and easiest to discern at low DA testing dilutions and short testing times (Figures 1B, S1A, and S1B).

To appreciate the net impact of conditioning, we calculated the learning index, reflecting the change in chemotaxis following conditioning compared to control. The learning index showed similar magnitude for the various training durations, both when DA + HCl was compared to DA alone (Figure 1C, left) or HCl alone (Figure 1C, right). Conditioning remained similar in strength for a range of training DA dilutions (Figures 1D and S1C), but increased with stronger HCl intensity (Figures 1E and S1D, smaller pH values). Very acidic HCl concentration (pH = 2) led to a significant decrease in chemotaxis, even for control worms exposed to HCl alone (Figure S1D), possibly due to damage from the high acidity. Varying DA testing dilutions (Figures 1F and S1E) or testing durations (Figures 1G and S1F) mainly altered baseline chemotaxis values, while preserving the detectability of decreased DA chemotaxis, with no significant effect on the learning index (Figures 1F and 1G). These results demonstrate that specific DA-HCl aversive conditioning can be induced rapidly and quantifiably across

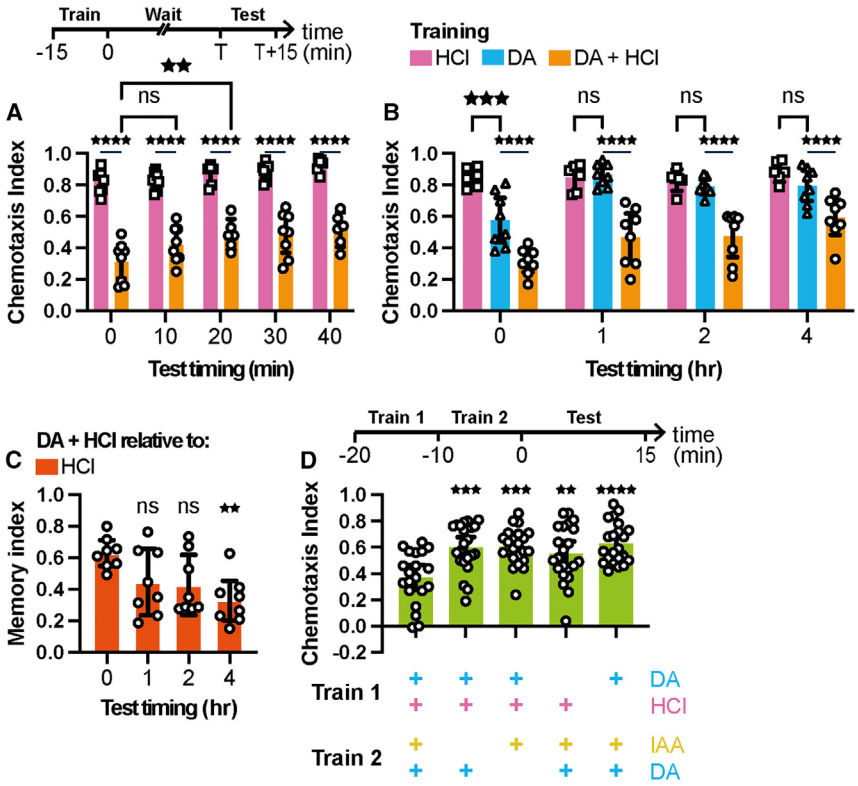

Figure 2. Memory retention of DA-HCl conditioning

(A–C) Changes in DA chemotaxis at variable test timing (T) post training. The Memory index (C), reflects the difference in chemotaxis after DA + HCl training compared to training with HCl alone.

(D) Second order conditioning (SOC) induced by DA and HCl coupling followed by isoamyl alcohol (IAA) and DA coupling, and then IAA chemotaxis testing. Error bars indicate mean ±95% confidence intervals. $^{**}p < 0.01$, $^{***}p < 0.001$, $^{****}p < 0.0001$. Details of the statistical analyses can be found in Data S1. Details of experimental parameters can be found in Table S2.

a broad parameter range, requiring only a few repetitions ($n = 6$ for most experiments) and avoiding potential system-wide effects. They also show distinct properties of adaptation and aversive conditioning, including their magnitude and dependency on training conditions.

Rapid aversive conditioning persists for at least several hours

So far, we have shown how conditioning leads to immediate behavioral changes. However, to assess memory retention, we examined chemotaxis at different time points post training. Chemotaxis tested 10 min post training was not significantly different from when tested immediately after training (Figure 2A). By 20 min after training, chemotaxis of DA + HCl conditioned worms slightly but significantly increased, indicating a modest memory decay (Figure 2A). At later time points memory remained stable (Figure 2A). The 10–20 min time window may reflect a possible transition between memory phases. Memory further persisted for at least 4 h (Figure 2B). To compare memory levels, we calculated the memory index (similarly to the learning index, with the learning index representing testing immediately following training and the memory index representing testing at later time points following conditioning), and found memory to remain comparable in size at the different time points, but showing a significant decay 4 h post training (Figure 2C). In contrast, adaptation was short-lived, undetectable by 1 h after DA training (Figure 2B, HCl alone vs. DA alone). Thus, adaptation and conditioning are further dissociated by differences in their persistence over time, further indicating that these two forms of behavioral plasticity are molecularly and behaviorally distinct processes.

Aversive conditioning can be extended to second order conditioning

Given the enduring impact of aversive conditioning (Figures 2A–2C), we explored the possibility that the altered valence of DA, following aversive conditioning, could function in itself as a secondary unconditioned stimulus (US2) when paired with a new conditioned stimulus (CS2). Such an effect is known as second order conditioning (SOC), documented in various species, from flies[21] to humans.[22] So far, SOC has not been reported in *C. elegans*.

We thus accompanied the initial DA + HCl training phase with a second training phase, in which we paired isoamyl alcohol (IAA), sensed by AWC neurons, as a second conditioned stimulus, CS2, with DA (sensed by AWA neurons), now acting as a second unconditioned stimulus, US2 (Figure 2D). Such training led to a significant decrease in IAA chemotaxis compared to control treatments, each lacking one of the

components of the two-phase procedure (Figure 2D). This result demonstrates the considerable impact of aversive conditioning, capable of transforming the conditioned response (reduced DA attraction) into a new unconditioned stimulus. It also further dissociates aversive conditioning from adaptation. This can be seen in the failure to condition IAA following the presentation of DA alone in the first training phase (Figure 2D, rightmost column), even though, like conditioning, it alters the valence of DA.

Temporal regulation of memory by specific sensory neurons

The CS (DA) and US (HCl) that we have chosen for the aversive conditioning procedure are mainly sensed by specific and distinct sensory neurons. HCl is primarily sensed by the nociceptive ASH neurons, while DA is detected by the AWA olfactory neurons. We were interested in examining the extent to which ASH and AWA may play a role in the process of memory consolidation following training. To this end, we employed a chemogenetic approach, silencing either ASH or AWA using a histamine-gated chloride channel, HisCl.[23–25] This channel enables transient silencing of target neurons upon external application of histamine, which is not endogenously produced by *C. elegans*.

We generated integrated ASH:HisCl and AWA:HisCl strains to explore the dependency of memory on the timing of neuron-specific silencing. To validate the specificity and effectiveness of silencing, we compared the effects of histamine application on behaviors that depend on AWA but not ASH, and vice versa. AWA, but not ASH, neurons detect low to mid-range DA concentrations, leading to attraction (Figure 3A, 1:1,000 dilution). Accordingly, application of 10 mM histamine suppressed this response in the AWA:HisCl strain (Figure 3B), but not the ASH:HisCl strain (Figure 3C) strain. Conversely, detection of high concentrations of DA by ASH, but not AWA, produces aversion (Figure 3A, 100% DA). Consistently, histamine application significantly decreased the repulsive response to this stimulus in the ASH:HisCl strain (Figure 3C), but not in the AWA:HisCl strain (Figure 3B). Histamine applied to the control strain (N2) lacking histamine-gated channels had no such effects (Figure 3A). Thus, histamine-based chemogenetic silencing could be used to specifically target AWA and ASH in the integrated strains.

To investigate the temporal dynamics of ASH and AWA in memory consolidation, worms expressing AWA:HisCl or ASH:HisCl were subjected to a 5-min pulse treatment with 10 mM histamine at specific time points post training, and then tested 1 h post training. We first examined the role of AWA olfactory neurons, required for sensing the conditioned stimulus (CS) diacetyl (DA). In order to distinguish between the effects of AWA silencing on learning and memory, as opposed to its possible impact on testing (the DA chemotaxis assay), we initially examined how AWA silencing without conditioning may affect DA chemotaxis. To this end, we performed mock training with only DDW, followed by histamine application at various subsequent time points, and tested DA chemotaxis 1 h after mock training. Indeed, AWA silencing at all time points within the 1-h interval between mock training and testing resulted in similarly reduced DA chemotaxis (Figure S2A). We thus examined whether AWA silencing between conditioning and testing had any additional disruptive effects on memory, beyond the basic baseline interference we noted (Figure S2A). We found that silencing AWA specifically 30 min post training, but not at other time points, resulted in significantly reduced memory (Figure 3D), exhibited by a lack of further chemotaxis suppression specifically at this timepoint, as opposed to other time points (Figure S2B). This finding suggests that AWA activity is required for 1 h memory formation and that this requirement has a very restricted temporal window.

For ASH:HisCl-expressing worms, treatment at time 0, but not later times, resulted in a significant decrease in memory (Figures 3E and S2C). This effect was not observed in control N2 worms lacking an exogenous histamine channel (Figures S2D and S2E). Next, we asked, at what stage does ASH silencing immediately after training begin to disrupt memory? To explore this, we applied histamine to ASH:HisCl worms immediately after training, and then tested chemotaxis at various subsequent time points. We initially observed an effect 45 min after training, and used this time point as a reference to gain a narrower temporal window and tighter control (Figures 3F–3H). Testing 10 min after training did not lead to any memory loss, compared to 45 min post histamine application (Figures 3F and S2F). However, by 15 min a significant disruption of memory could be observed in ASH:HisCl worms but not in N2 worms (Figures 3G, 3H, and S2G–S2J). Thus, the memory can be separated into an early phase, independent of ASH activity immediately post training, and lasting up to about 10 min after training, and a later, prolonged, ASH-dependent phase, beginning about 15 min post training. Together, these results indicate that beyond their direct role in sensing DA and HCl during conditioning, ASH and AWA neurons participate in various phases of memory, with distinct temporal signatures.

Temporal impact of transcription and translation on aversive conditioning

Previous studies in *C. elegans*[26,27] have highlighted the roles of transcription and translation in memory consolidation. To further explore the dynamic profile of gene activation and protein synthesis during aversive conditioning, we used actinomycin D (50 μg/mL) and cycloheximide (0.8 mg/mL), to systemically block transcription and translation, respectively.[26] We subjected worms to a 5 min pulse treatment of either drug at specific time points post training, and assessed the effects on chemotaxis 1 h after training (Figures 4 and S3).

Inhibiting transcription at 0 and 15 min after training resulted in a significant decrease in memory compared to control (Figures 4A and S3A). Blocking at later time points had no such effect. Disrupting translation immediately and 30 min after training, but not at 15- or 45-min post training, resulted as well, in a significant decrease in memory (Figures 4B and S3B).

To pinpoint when memory becomes dependent on transcription and translation, we repeated the blocking of these processes at time 0 and then tested memory at time points 30 and 45 min post training. Our results showed that memory becomes transcription- and translation-dependent from between 30 and 45 min after training (Figures 4C, 4D, S3C, and S3D). Interestingly, blocking translation at time 0 and testing at time 30 showed no significant decrease in memory (Figures 4E and S3E, block timing 0 min), whereas blocking translation at time 30 and testing at time 60 did exhibit a significant decrease in memory, despite the similar delay between blocking and testing (Figures 4E and

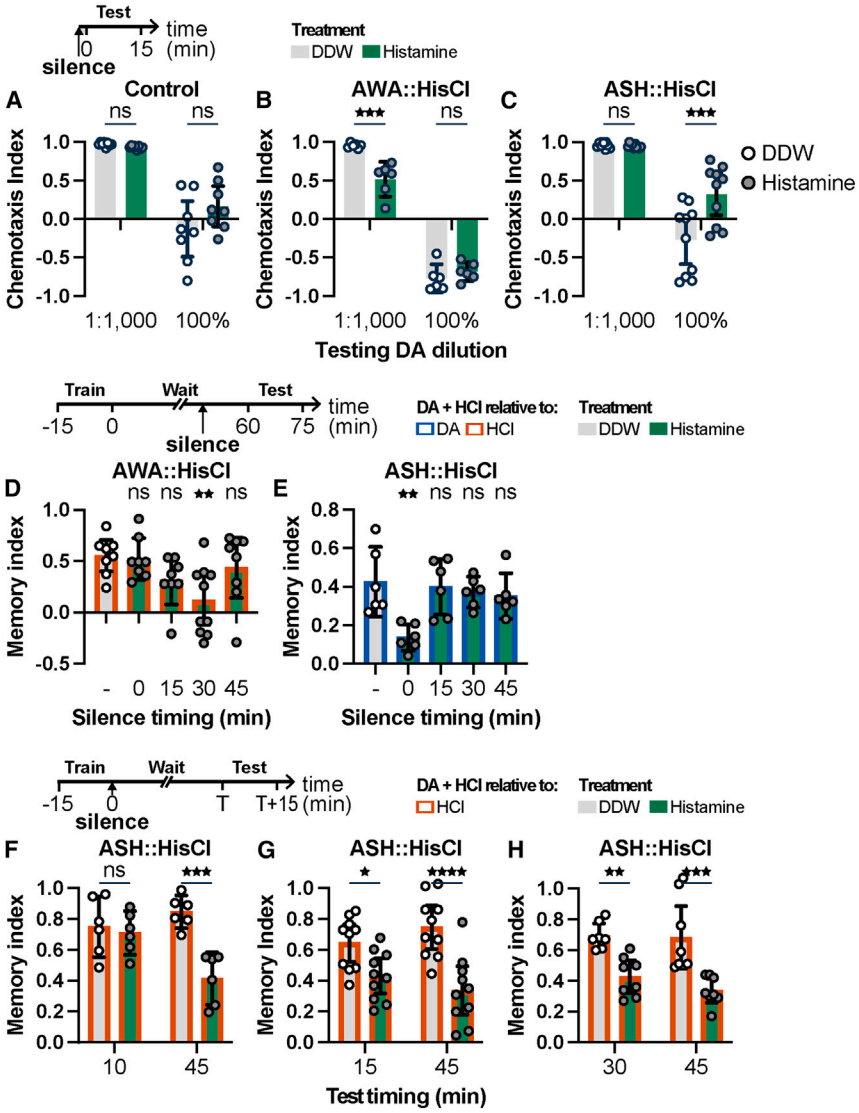

Figure 3. Sensory neuron silencing differentially disrupts DA-HCl conditioning

(A–C) Application of 10 mM histamine for 3 min to control worms (A), worms carrying the histamine-gated chloride channel (HisCl) in the AWA olfactory sensory neurons (B), or the ASH nociceptive neurons (C) during chemotaxis to moderate (3 μL 1:1,000) or intense (10 μL 100%) DA dilutions.

(D and E) Application of 10 mM histamine to worms carrying AWA:HisCl (D) or ASH:HisCl (E) at various time points between training and testing.

(F–H) Application of 10 mM histamine to worms carrying ASH:HisCl immediately post training with variable test timing (T). Error bars indicate mean ±95% confidence intervals. $^{\star}p < 0.05$, $^{\star\star}p < 0.01$, $^{\star\star\star}p < 0.001$, $^{\star\star\star\star}p < 0.0001$. Details of the statistical analyses can be found in Data S1. Details of experimental parameters can be found in Table S2.

S3E, block timing 30 min). This further illustrates the importance of the timing of translation relative to conditioning for proper memory consolidation. Overall, the dynamics we observe suggest the existence of distinct waves of transcription and translation of memory-related genes within the 1 h time frame. Together, our results resolve a transition point between immediate and extended phases of memory, based on the reliance on transcription and translation.

RNA sequencing unveils dynamic temporal gene expression patterns during memory consolidation

Since transcription plays an important role in the process of memory formation and consolidation, specifically soon after training (Figure 4A), we wished to explore in further detail gene expression changes at different time points following conditioning. To this end we sequenced total RNA collected from conditioned (DA + HCl) vs. control (HCl or DA alone) worms, 20 and 60 min post training, as well as from conditioned worms 40 min post training. This produced seven experimental groups (four control and three conditioned), each including three biological replicates. We reasoned that analyzing total RNA expression would enable the coverage of a broad range of genes, expressed in diverse cells

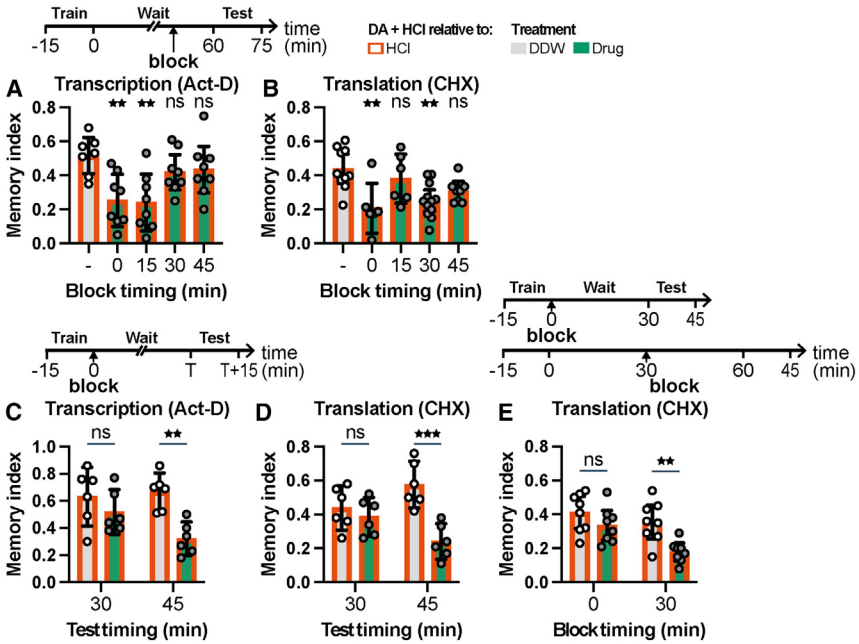

Figure 4. Transcription and translation inhibition differentially disrupts DA-HCl conditioning

(A and B) Application of 50 μg/mL actinomycin D (Act-D) (A) or 0.8 mg/mL cycloheximide (CHX) (B) at various time points between training and testing.

(C and D) Application of Act-D (C) or CHX (D) immediately post training with variable test timing (T).

(E) Application of CHX at two time points after training and 30 min prior to testing. Error bars indicate mean ±95% confidence intervals. $^{\star}p < 0.05$, $^{\star\star}p < 0.01$. Details of the statistical analyses can be found in Data S1. Details of experimental parameters can be found in Table S2.

and tissues, even at the expense of weakened signal strength, especially for ubiquitous or multi-purpose genes with selectively altered expression only in small subsets of cells, for which differential expression should be more challenging to detect.

Principal Component Analysis (PCA) of the gene expression data showed a remarkable temporal separation along the first principal component (Figure 5A; PC1), suggesting salient overall gene transcription dynamics at different time points after training. Differences between conditioning and control training were also discernable, but were much more subtle (Figure 5A).

We identified post conditioning differentially expressed genes (DEGs), using edgeR (see STAR Methods). We averaged for this purpose the expression levels of the two control conditions (DA alone and HCl alone; Figure 5B). As an inclusion criterion we considered as DEGs genes with a *p* value smaller than 0.05 and a percent change greater than 15% (Figure 5B; see STAR Methods). According to this criterion ~4% of the mapped genes showed altered expression levels 20 min after training (Table S3), and ~6% of the genes changed expression 60 min after training (Figure 5B; Table S4). Altogether, a total of 1,381 DEGs met our inclusion criteria (Table S5). Only a small fraction of genes were differentially expressed both 20 and 60 min post training (Figure 5C), further emphasizing the sequential temporal nature of memory consolidation that can be separated according to the identity of the genes involved in each part of the process. We also conducted a DEG analysis pooling all conditioned samples vs. all control samples, ignoring the time variable. This analysis yielded additional 333 DEGs that met our inclusion criteria (Table S6).

To visualize temporal changes in gene expression, we performed hierarchical clustering of the normalized expression intensities of the 1,381 selected DEGs (Figure 5D), taking into consideration the 40 min time point not included thus far in the analysis. Dividing the data into four clusters (Table S7) showed distinct temporal expression patterns (Figures 5D and 5E). Cluster 1 and 2 exhibited transcripts showing a slow and stable upward trend mostly at relatively late time points post-conditioning (Figure 5E). Gene Ontology (GO) enrichment analysis (Table S1) of Cluster 2 included terms related to cell communication, signal transduction, and tissue morphogenesis, which could be associated with plasticity. Cluster 3 exhibited a rapid increase in transcript expression 20 min after conditioning (Figure 5E), with enriched GO terms related prominently to stress as well as to metabolism (Table S1). Conversely, Cluster 4 displayed an overall downward trend, with GO enrichment terms linked to proteolysis, metabolism and to some extent also to stress.

Altogether, DEG analysis revealed dynamic temporal patterns of gene expression that could be paralleled to different memory phases.

Putative core memory genes

Our current DEG results complement previous transcriptional profiles attained in conjunction with *C. elegans* associative learning.[26,27,29] The various studies differ considerably in the training regimes applied, methods of transcript probing, timing of RNA collection, tissue enrichment and genetic background. Their outcomes are thus not directly comparable. However, shared genes between the datasets could represent putative core memory genes. We thus examined the 1,381 DEGs from our current study (Table S5) in comparison with 1,524 DEGs previously

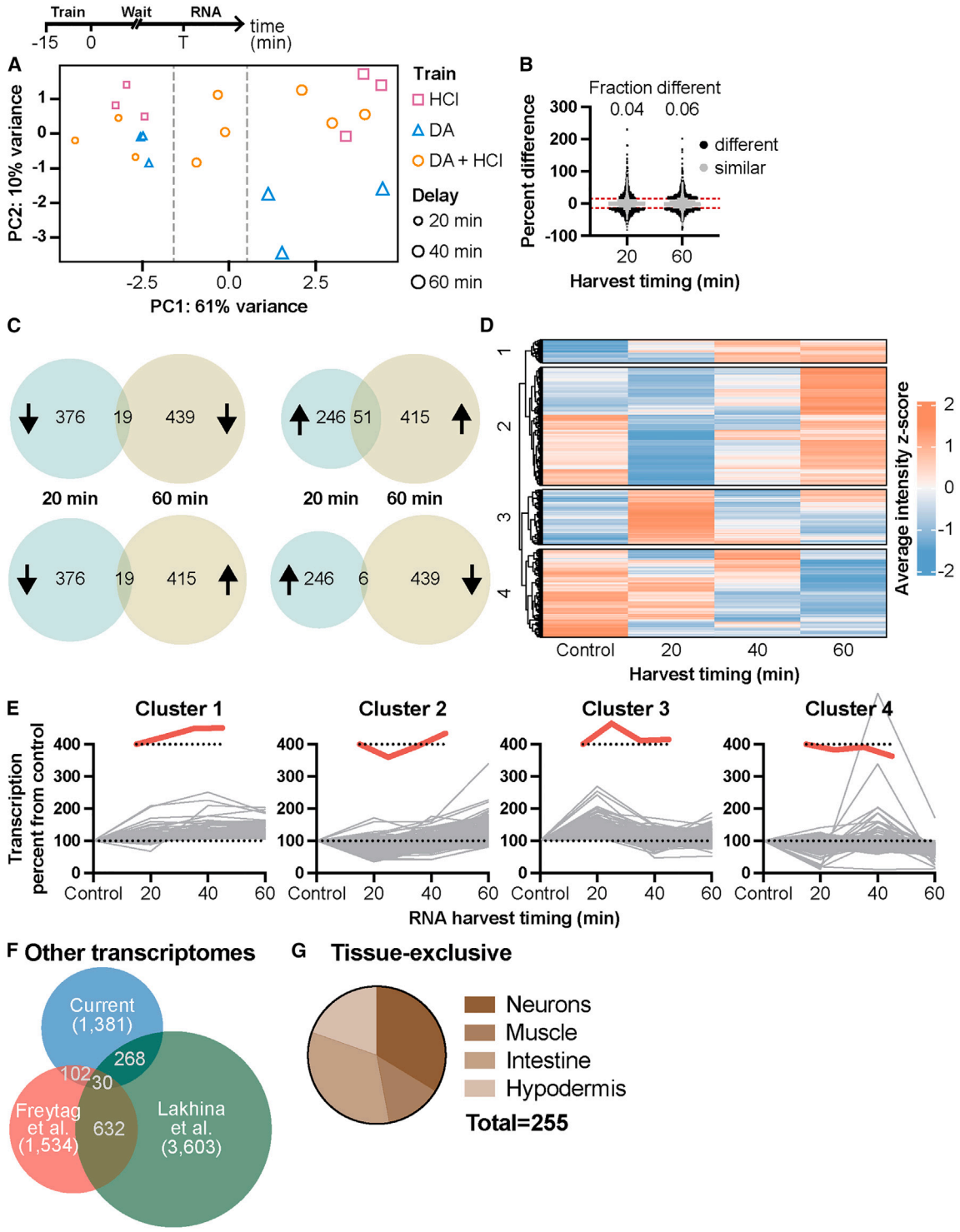

Figure 5. Temporal transcriptional profile following aversive conditioning

(A) Principal Component Analysis (PCA) projection of gene transcript levels at specific time points (T) after different training regimes (control vs. conditioning). For each experimental group 3 independent biological samples are shown.

(B) Percent difference in transcript levels between conditioning (DA + HCl) and the average of the two control treatments (DA and HCl alone). Each dot represents a different gene. Black dots are genes with $p < 0.05$ and a percent fold-change greater than 15% (red dotted lines). Gray dots are genes that did not pass these inclusion criteria (rejected).

Figure 5. *Continued*

(C) Number of genes showing significant difference in expression (DEGs) between conditioning and control (B) at both 20- and 60-min delay after training. Arrows indicate downregulated (↓) or upregulated (↑) expression.

(D) Heatmap showing 4 clusters of the DEG average intensity *Z* score, including the 40 min time point and pooled control values.

(E) DEG expression levels as percent from the average of all controls, divided into 4 clusters. Insets show scaled-up average expression levels of each cluster relative to control. (F) Overlap between DEGs from the current study, Freytag et al.,[26] and Lakhina et al.[27]

(G) Distribution of tissue-enriched genes in the DEG list from our current study between different tissues.[28]

identified following aversive conditioning between diacetyl and food deprivation.[26] We found 102 overlapping genes in these two datasets (Figure 5F). The intersection between these shared genes and a set of genes previously identified as related to appetitive conditioning between butanone and food,[27] narrowed the list down to only 30 genes (Figure 5F; Table S8). Many of the genes in this shared list have not been characterized, and for known genes, the function and expression patterns were considerably variable (Table S8). Also, there were no noticeable links between these genes and memory. Thus, it is difficult to point at common patterns within this convergent gene set. It is worth recalling that even within our own study we found only minimal overlap in DEGs between the 20 and 60 min time points (Figure 5C). Therefore, it is not surprising that the number of genes shared with other datasets collected at very different time points following very different training procedures, is so small. Thus, the memory-related gene signature is likely highly dependent on the temporal window following conditioning.

We further sought to explore potential similarities in GO terms across the different datasets. Even though certain genes may not have been identified as DEGs in all three studies, we hypothesized that common underlying pathways or molecular processes could still exist. To detect relatively specific functional classes, we focused on category 3 GO terms from WormCat (see STAR Methods). Several specific terms were identified (Table 1), including those related to signaling, pathogen stress responses, metabolism, extracellular materials, and proteolysis. The number of intersecting genes associated with each GO term across all three datasets was minute (e.g., Figure S4A; Table S9), as expected from the generally small overlap between DEGs (Figure 5F). At the same time, the union of genes corresponding to each GO term from the 3 datasets covered a considerable proportion of the total number of genes associated with that term (e.g., Figure S4B; Table S9). Thus, similar molecular and cellular functions may be instantiated by distinct gene subsets under different learning conditions and along different stages of memory formation and consolidation.

We further studied the expression patterns of the DEGs we had detected. To this end, we considered genes previously found to be highly enriched in one of four *C. elegans* main tissues: neuron cells, muscle cells, intestine and hypodermis.[28] We identified amongst our DEGs 255 such genes. Notably, gene expression was not unique to neuronal tissue (Figure 5G; Table S10), suggesting that even circumscribed non-systemic learning, as we have applied, may still involve substantial interaction with non-neuronal genes.

Variable memory dynamics in a sample mutant library

To complement the broad coverage provided by transcriptional analysis, we sought to probe the effects of particular gene mutations on aversive conditioning, and to examine the extent to which genetic background may impact the temporal profile of memory. To this end, we selected a sample of 29 genes from both sets of transcriptional results: 17 genes that met our inclusion criteria, and 12 additional genes that showed considerable fold change (FC) relative to control, even though they were not significant in the DEG analysis, but did exhibit significant differential expression in RT-qPCR analysis (see below). These genes represent together diverse functions and expression patterns (Table 2). We first performed reverse transcription quantitative PCR (RT-qPCR) to verify memory-related changes in transcript abundance following conditioning 20 or 60 min post training (Figure S5). All genes tested (except for *hsp-16.2*) showed significant changes in transcript levels relative to both DA alone and HCl alone at one of the two timepoints (Figure S5).

We subjected strains carrying mutations in the selected genes to DA + HCl conditioning, and tested their chemotaxis 0, 1 and 4 h post training, with reference to N2, the control strain (Figure 6A). To enable qualitative comparison between the mutant strains, we calculated the memory index of each mutant as a fraction of its value at time 0. We found considerable variability in memory levels across time points (Figure 6B, Top). Unlike N2, whose memory index showed a significant decrease by 4 h post training (Figure 6A), 18 out of the 29 mutant strains showed stable memory with no significant differences between the various time points (Figure 6B, 'Stable'; Figure S6A). 4 mutant strains showed a significant increase in memory index at the 1 h time point (Figure 6B, '1 h increase'; Figure S6B), 4 mutant strains displayed increased memory 4 h after training (Figure 6B, '4 h increase'; Figure S6C), and 3 mutant strains showed a significant decrease in memory index at 1 h post training (Figure 6B, '1 h decrease'; Figure S6D). The particular impact of each gene on specific memory phases will require further investigation.

Finally, we considered homologs of these tested genes and examined which ones had been previously linked to memory, synaptic plasticity, neurodegenerative disease or overall neuronal function. We found that roughly half of the 29 genes corresponded to such processes in other species (Table 3).

Mutant strains with extended memory

Having identified multiple mutant strains with sustained memory 1 and 4 h post training, we wished to extend our analysis and examine more prolonged memory retention. We thus tested chemotaxis 18 h post training in N2 and 8 of the mutant strains. By 18 h, memory of the N2 control strain fully decayed, as well as in 4 mutant strains (Figure S6E). However, in the other 4 mutant strains, memory was still detectable even 18 h after training (Figure 6C). Thus, certain genes may actively regulate forgetting. Further exploration of the sample mutant strains

Table 1. Shared category 3 gene ontology (GO) terms in our current DEG list and 2 previous DEG datasets

GO term	Current	Freytag et al.[26]	Lakhina et al.[27]
Signaling: hedgehog-like	3.80E-04	1.49E-07	9.68E-05
Transcription factor: bZIP	1.40E-03	1.42E-03	1.38E-02
Stress response: pathogen: unassigned	5.70E-03	5.81E-03	6.47E-10
Metabolism: lipid: beta oxidation	2.90E-02	2.94E-02	5.18E-10
Extracellular material: matrix	3.67E-02	3.14E-05	4.59E-06
Extracellular material: collagen	1.89E-04	2.31E-02	3.25E-32
Extracellular material: cuticlin	2.58E-02	1.02E-08	6.07E-03
Proteolysis proteasome: E3: F box	3.38E-04	1.12E-05	6.66E-09
Transmembrane protein: unassigned	7.30E-07	4.87E-06	3.61E-07
Unassigned: prion domain	2.32E-06	4.20E-02	4.39E-02
Unassigned: regulated by multiple stresses	3.14E-22	4.31E-17	4.83E-48

Enrichment *p*-value shown for each term in each dataset.

that we have tested (Figure 6B, bottom) and other DEGs (Figure 5B), could provide valuable insights into the molecular regulation of various processes underlying memory formation, consolidation and forgetting[8,9,24,51].

DISCUSSION

We have demonstrated a rapid and highly effective form of associative learning in *C. elegans*, and a capacity in this animal for robust conditioning, extendible even to second order conditioning. Associative learning has been studied quite extensively in *C. elegans*,[12,13,52–55] employing diverse protocols, typically tailored to evoke either short-, intermediate-, or long-term memory.[56] Our unified approach made it possible to systematically delineate the temporal dynamics of distinct memory phases and the transition points between them.

Temporal dissection of memory transition

Our findings enabled to partition post-conditioning associative memory into distinct phases with clear transition points between these phases (Figure 7). First, we revealed that immediately and up to 15 min post conditioning, memory is independent of transcription, translation, or the activity of ASH or AWA sensory neurons (Figure 7). However, after 15 min, memory becomes dependent on ASH sensory neuron activity (Figure 3G). Interestingly, we observed a difference in chemotaxis between 10 and 20 min post conditioning relative to 0 min post conditioning (Figure 2A). This partial recovery of chemotaxis may signify the onset of a form of short-term forgetting, suggesting a first detectable transition between memory phases. Second, by 45 min post conditioning, memory becomes dependent on AWA sensory neuron activity, in addition to ASH activity (Figures 3F–3H), as well as on transcription and translation processes (Figures 4C and 4D), indicating a second transition between memory phases. Third, after stably persisting for at least 2 h post conditioning (Figure 2B), memory gradually decayed, with significant decreases observed 4 h post conditioning (Figure 2C), and then, fourth, complete forgetting 18 h post conditioning (Figure 6C). Thus, we defined the initial 15 min post-conditioning as short-term memory (STM), followed by 15–45 min as intermediate-term memory (ITM),[6] and 45 min onwards as long-term memory (LTM), with forgetting commencing approximately 2 h post-conditioning (Figure 7).

Consistent with previous studies,[18] STM showed transcription- and translation-independence, whereas LTM exhibited transcription- and translation-dependance. ITM is generally considered to be transcription-dependent, but its dependence[57] or independence[11,58] on translation varies between studies. In our assay, the ITM phase we identified was dependent only on ASH activity, and not on transcription or translation. These differences could be due to more nuanced unidentified memory phases, each comprising unique transcription and translation signatures.

ASH and AWA sensory neurons participate in memory consolidation

ASH and AWA neurons detect the particular sensory stimuli present during conditioning. Our findings reveal that these sensory neurons play also an additional important role during memory consolidation. We found ASH sensory neuron activity to be essential for ITM and LTM (Figures 3E, 3G, and 3H), and AWA sensory neuron activity to be required 30 min post conditioning, specifically for LTM (Figure 3D). This is somewhat reminiscent of the distinct involvement of different brain regions at varying time points in memory consolidation in more complex systems.[59]

We also find certain correspondence between the timing and the impact on memory of ASH and AWA activity and transcription and translation. First, although silencing either ASH or AWA sensory neurons had an immediate impact on chemotaxis (Figures 3B and 3C), the effects on memory were delayed (Figures 3D–3H), resembling the delayed outcome of transcription and translation inhibition (Figures 4A–4D). This delay could be due to downstream cellular processes linking each treatment to particular memory phases. Second, neither ASH or AWA activity, nor transcription and translation, were necessary for STM, and all were required for LTM (Figure 7). Finally, the requirement for

Table 2. List of mutant strains used for analysis

Strain	Mutation	General function	Key expression
PS8636	*ins-10(sy1437)*	Insulin-related	Multiple tissues
PS8313	*nlp-79(sy1268)*	Neuropeptide	Neurons
RB2040	*frpr-18(ok2698)*	Neuropeptide receptor	Neurons and elsewhere
VC1392	*zip-5(gk646)*	Transcription factor	Neurons, intestine
VC475	*hsp-16.2(gk249)*	Heat shock protein	Multiple tissues
VC3113	*tax-4(ok3771)*	Cation channel	Sensory neurons
VC4610	*H12I13.1(gk5680)*	Proteolysis?	NSM neuron
RB2604	*W02G9.4(ok3626)*	Unestablished	Multiple tissues
RB1048	*gcy-32(ok995)*	GTP→cGMP	Oxygen neurons
VC2625	*T19D12.5(gk1136)*	Unestablished	–
NL1142	*gpa-8(pk345)*	G protein	Neurons
VC2171	*tkr-1(ok2886)*	GPCR?	Neurons
RB1077	*rgs-10(ok1039)*	Signaling regulator	Multiple tissues
RB1417	*cul-6(ok1614)*	Ubiquitination	Multiple tissues
VC1386	*nhr-207(gk632)*	Nuclear receptor	Multiple tissues
VC2916	*maf-1(gk1242)*	Unestablished	Multiple tissues
CZ9957	*gtl-2(n2618)*	TRPM channel	Multiple tissues
RB1289	*npr-18(ok1388)*	Neuropeptide receptor	Neurons and elsewhere
PS9192	*mgl-1(sy1623)*	Glutamate GPCR	Neurons
PS8315	*npr-29(sy1270)*	Putative receptor	Neurons
VC1453	*unc-4(gk668)*	Transcription factor	Neurons
RB1455	*nekl-1(ok1662)*	Phosphorylation?	Neurons
VC2434	*skr-5(ok3068)*	Ubiquitination?	Multiple tissues
CB518	*bli-5(e518)*	Cuticle biosynthesis	Multiple tissues
RB1996	*try-11&8(ok2641)*	Proteolysis?	Germ line
RB2343	*try-13(ok3179)*	Proteolysis?	Neurons, germ line
VC2606	*F22F1.2(ok3350)*	Unestablished	Neurons
RB681	*cat-1(ok411)*	Vesicular transporter	Neurons and elsewhere
PS8865	*lgc-42(sy1550)*	Ligand-gated channel	Neurons

General function and key expression pattern derived from www.wormbase.org[30] and www.uniprot.org.[31]

transcription, translation, and ASH activity immediately post training is suggestive of previous findings demonstrating a narrow window for disrupting memory consolidation immediately post learning, through the inhibition of mRNA[60] or protein synthesis,[61,62] neuronal activity,[62] or mTOR (mechanistic target of rapamycin) kinase,[63,64] as well as specific brain lesions.[65]

Additionally, the time-dependent relationship observed between ASH and AWA for LTM – with ASH activity required immediately post-training, while AWA activity is required only 30 min post-training – may correlate with studies showing that different brain regions become essential for memory consolidation at various time points post-conditioning.[66] Building upon this, we propose a possible sequential relationship between sensory neurons and transcription and translation, wherein ASH may serve as the initiator of transcription and translation, followed by AWA participation.

Temporal and spatial patterns of gene expression

Investigating temporal gene expression patterns in treated worms showed a strong time-dependent effect of training on the levels of gene expression, across all treatments (Figure 5A). Notably, even within this dynamic and distributed transcriptional response, we were able to define a large set of putative genes with differential expression between conditioned and control worms (Figure 5C), and to observe diverse temporal profiles of memory dynamics among different mutant strains (Figure 6B). Thus, even highly specific, brief and restricted conditioning leads to multiple diverse waves of gene activity.

Moreover, although the training procedure we applied was circumscribed, involving particular isolated stimuli detected by specific identified sensory neurons, the distribution of detected genes across tissues and cells was rather broad (Figure 5G; Table 2). It has previously been shown in *C. elegans* that salient transient changes in environmental conditions, including even brief (15 min) heat shock, for

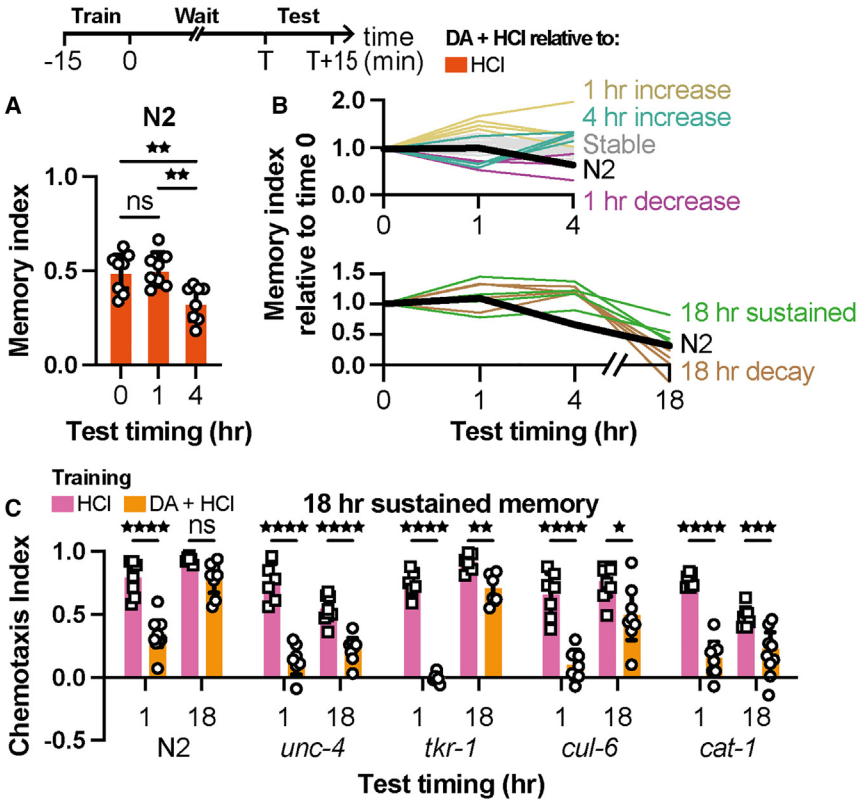

Figure 6. Altered memory retention profiles in *C. elegans* strains with diverse genetic backgrounds

(A) N2 memory index at T = 0, 1 and 4 h post training.

(B) Memory index at T = 0, 1 and 4 h post training (top) for 29 mutant strains, and 18 h post training (bottom) for 8 mutant strains. N2 values represented by the thick black thick line. Values are presented as fraction relative to time 0.

(C) Chemotaxis at T = 1 and 18 h after training of mutant strains showing sustained memory. Error bars indicate mean ±95% confidence intervals. $^{\star}p < 0.05$, $^{\star\star}p < 0.01$, $^{\star\star\star}p < 0.001$, $^{\star\star\star\star}p < 0.0001$. Details of the statistical analyses can be found in Data S2. Details of experimental parameters can be found in Table S2.

example, can elicit cell non-autonomous systemic responses requiring initial detection of the temperature shift by dedicated sensory neurons.[67] It has also been shown that non-autonomous signaling from the hypodermis, for instance, facilitates short-term associative learning in *C. elegans*,[68] further emphasizing how learning may involve broad physiological processes comprising diverse cells and tissues.

Comparison of memory-related gene ontology terms with previous studies

When comparing the genes we identified as DEGs in the current study to previous DEGs related to *C. elegans* learning and memory,[26,27] we found a very small overlap (Figure 5F). This was consistent with the considerable differences in gene expression that we observed even within our own study between 20 min and 60 min post training (Figure 5C). The dynamic temporal nature of memory-related gene expression could be an important factor contributing to this diversity. To investigate broader connections between the datasets, we compared also category 3 WormCat gene ontology (GO) terms derived from the different DEGs. Interestingly, we identified 11 shared GO terms (Table S9), some of which appeared to be especially interesting in the context of memory (Figure S4).

For instance, the term "Signaling: Hedgehog-like" refers to proteins containing the warthog (wrt), groundhog (grd), ground-like (grl) genes, and Patched Related family (ptr) proteins. Although this protein family is not directly linked to memory, there is evidence that CREB, an important player in neurodevelopment and plasticity,[69] controls reproductive aging through Hedgehog-like proteins.[70] The potential connection between these proteins and memory remains to be explored. An additional shared GO term, "Proteolysis proteasome: E3: F box", can be linked to memory and plasticity.[71,72] In particular, F box proteins serve as substrate adaptors in ubiquitin ligase complexes, mediating the proteasomal degradation of a wide range of regulatory proteins.[73] Finally, "Transcription factor: bZIP", relates to a large family of transcription factors containing the bZIP domain. These proteins are involved in various developmental processes, including dendritic cell development, myeloid differentiation, and brain development. Several members of this family, such as Jun-B and CREB,[74] have been associated with memory formation.

Table 3. Mutant gene homologs with reported roles in learning and memory

Gene	Homolog	Roles in memory and neuronal function
tax-4	CNGA3	Synaptic plasticity[32]
W02G9.4	CSMD3	Synaptogenesis[33]
gcy-32	Gucy1b3	Spatial learning, age-sensitive[34]
T19D12.5	TTBK1	Neurodegeneration[35]
gpa-8	GNAO1	Epilepsy and movement disorders[36]
tkr-1	TACR1	Downregulated in fear conditioning[37]
	TACR3	Memory age-sensitive[38]
rgs-10	RGS3	Neurotransmission, schizophrenia[39]
cul-6	CUL1	Differential expression in Alzheimer's disease[40]
nhr-207	NR1H3	Amyloid-β clearance (neurodegeneration)[41]
gtl-2	TRPM3	Memory[42]
npr-18	SSTR5	Neuromodulation, cognition[43]
mgl-1	GRM3	Hippocampus-dependent memory, working memory, schizofrenia[44,45]
unc-4	ARX	Neurodevelopment[46]
skr-5	SKP1	Ubiquitination[47]
cat-1	VMAT	Possible gaiting of memory consolidation[48]
lgc-42	GLRA1	Memory, synaptic plasticity, autism spectrum disorder[49]
try-8	HGFAC	Neuroprotective effect in Alzheimer's disease[50]

This finding suggests that rather than a core set of genes being exclusively required for memory, the process of memory formation and consolidation may involve the selective timing-dependent engagement and reconfiguration of multiple, overlapping and distributed gene networks that are recruited based on specific demands of the memory process as well as particular environmental context.

Comparison of memory-related gene homologs

Many of the mutant strains that we tested showed altered patterns of memory formation and consolidation (Figure 6 and S6). Interestingly, several of these mutant strains showed altered memory patterns reminiscent of their corresponding gene homologs (Table 3). For example, *mgl-1* mutants showed weaker short-term memory compared to long-term memory (Figure S6B). Correspondingly, *mgl-1* homologs, GRM2/3, exhibit impaired short-term memory.[44] *tkr-1* mutants showed delayed forgetting, enabling memory to persist even 18 h post training (Figure 6C and S6C). At the same time, activation of the NK3-Receptor (encoded in humans by the TACR3 gene), a *tkr-1* homolog, improved learning and memory in aged rats.[38] Similarly, *cat-1* mutants exhibited persisting memory 18 h post training (Figure 6C), while downregulation of the *cat-1* homolog, VMAT, has been shown to enhance long-term memory formation in the fruitfly.[48] This resemblance between homologous proteins highlights a possible conservation of memory-related genes across species.

An additional set of mutants that caught our attention belong to the *try* family (trypsin-like proteases).[75] While not much is known about this protein family, and we were not able to establish a direct link between these mutants, their homologs, and learning or memory from the literature, their structure and GO terms suggest involvement in proteolysis (Table 2), which is thought to play an important role in memory and synaptic plasticity,[71,72] although these mutants have not been extensively studied in this context. In our analysis, we observed that *try-8*, *try-11*, and *try-13* exhibited increased mRNA abundance following conditioning compared to HCl and DA (Figures S5A and S5B). However, their memory retention profiles diverged (Figures S6C and S6D). The *try-8*; *try-11* double mutant showed reduced LTM (1 h post training) but delayed forgetting (4 h post training, Figure S6C), while *try-13* displayed a more pronounced reduction in LTM alongside accelerated forgetting (Figure S6D). These findings suggest that the *try* genes may regulate each other to modulate memory retention and forgetting.

Future uses for the conditioning protocol

Our conditioning protocol provides an effective platform for rapidly and robustly inducing associative memory in *C. elegans*, enabling the demonstration of how subsequent sequential processes of memory consolidation, and ultimately, forgetting, can be discerned and analyzed at the behavioral, neuronal and genetic levels using a single simple training procedure. This platform may serve as a powerful and rich launch pad for future investigation of memory formation and consolidation in multiple directions, including the dynamic participation and interaction among different neurons and between neurons and other tissues; the involvement of diverse genes and gene networks, such as identified in

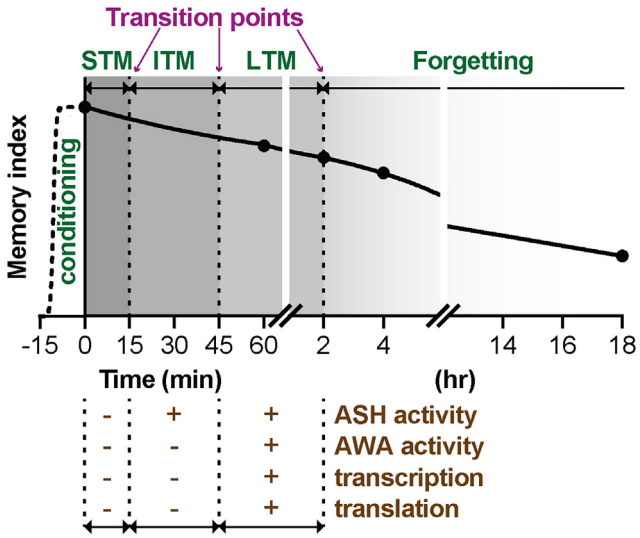

Figure 7. Memory phases summarized

Following conditioning, worms initially modify their behavior, transitioning (dotted lines) between discernable memory phases: short-term memory (STM), intermediate-term memory (ITM), long-term memory (LTM), and subsequently, a forgetting process. Each memory phase shows distinct dependencies ('+' signs at bottom) on ASH or AWA post-conditioning neuronal activity, transcription or translation.

our work, in various stages of the memory process; and higher order forms of conditioning, such as second order conditioning that we have currently demonstrated.

Limitations of the study

Like any conditioning procedure, the one developed for our study comprises specific features that may not necessarily capture the entire process underlying learning and memory. In particular, we included a 2-h food deprivation step immediately prior to training, as performed in earlier studies.[11,76,77] Absence of food has been previously shown to enhance conditioning,[76] as well as other forms of learning in *C. elegans*.[78] Although worms were equally exposed to the same pre-starvation treatment under all experimental conditions (starvation did not serve as an unconditioned stimulus), we cannot rule out possible interactions between stress and metabolic responses to starvation and learning and memory processes. This may especially affect gene expression. It will be important in future work to study the extent to which prior experience impacts learning and memory, and its possible interactions with this process.

RESOURCE AVAILABILITY

Lead contact

Further information and requests for resources should be directed to and will be fulfilled by the Lead Contact, Ithai Rabinowitch (ithai.rabinowitch@mail.huji.ac.il).

Materials availability

Strains generated in this study are available from the lead contact upon reasonable request.

Data and code availability

- All data generated in this study are available as Supplemental tables. In addition, RNA-seq data have been deposited at NCBI and are publicly available as of the date of publication. Accession numbers are listed in the key resources table.
- This paper does not report original code.
- Any additional information required to reanalyze the data reported in this paper is available from the lead contact upon request.

ACKNOWLEDGMENTS

This work was supported by Israel Science Foundation Grant 1465/20 and by the Horizon Europe, PathFinder European Innovation Council Work Programme under grant agreement No 101098722. Views and opinions expressed in this article are those of the authors only and do not necessarily reflect those of the European Union or European Innovation Council and SMEs Executive Agency (EISMEA). Neither the European Union nor the granting authority can be held responsible for them. We are grateful to the CGC, which is funded by NIH Office of Research Infrastructure Programs (P40 OD010440), the *C. elegans* Gene Knockout Project at the Oklahoma Medical Research Foundation, which was part of the International *C. elegans* Gene Knockout Consortium and to Dr. Yun Zhang and Dr. Cornelia Bargmann for strains.

AUTHOR CONTRIBUTIONS

Conceptualization, N.C. and I.R.; Formal Analysis, N.C. and I.R.; Investigation, N.C. and I.R.; Writing, N.C. and I.R.; Visualization, N.C. and I.R.; Supervision, I.R.; Funding Acquisition, I.R.

DECLARATION OF INTERESTS

The authors declare no competing interests.

DECLARATION OF GENERATIVE AI AND AI-ASSISTED TECHNOLOGIES

During the preparation of this work, the authors used ChatGPT in order to edit some of the text. After using this tool or service, the authors thoroughly reviewed and edited the content as needed and take full responsibility for the content of the publication.

STAR★METHODS

Detailed methods are provided in the online version of this paper and include the following:

- KEY RESOURCES TABLE
- EXPERIMENTAL MODEL AND STUDY PARTICIPANT DETAILS
  - Caenorhabditis elegans
- METHOD DETAILS
  - Behavioral assays
  - Transcriptional profiling
- QUANTIFICATION AND STATISTICAL ANALYSIS

SUPPLEMENTAL INFORMATION

Supplemental information can be found online at https://doi.org/10.1016/j.isci.2024.111147.

Received: May 30, 2024
Revised: August 26, 2024
Accepted: October 7, 2024
Published: October 10, 2024

REFERENCES

1. Gross, K., Pasinelli, G., and Kunc, H.P. (2010). Behavioral plasticity allows short-term adjustment to a novel environment. Am. Nat. *176*, 456–464. https://doi.org/10.1086/655428.
2. Bhat, A., Greulich, M.M., and Martins, E.P. (2015). Behavioral plasticity in response to environmental manipulation among zebrafish (Danio rerio) populations. PLoS One *10*, e0125097. https://doi.org/10.1371/journal.pone.0125097.
3. Pearce, J.M., and Bouton, M.E. (2001). Theories of associative learning in animals. Annu. Rev. Psychol. *52*, 111–139. https://doi.org/10.1146/annurev.psych.52.1.111.
4. Sasakura, H., and Mori, I. (2013). Behavioral plasticity, learning, and memory in C. elegans. Curr. Opin. Neurobiol. *23*, 92–99. https://doi.org/10.1016/j.conb.2012.09.005.
5. Nadel, L., Hupbach, A., Gomez, R., and Newman-Smith, K. (2012). Memory formation, consolidation and transformation. Neurosci. Biobehav. Rev. *36*, 1640–1645. https://doi.org/10.1016/J.NEUBIOREV.2012.03.001.
6. Rosenzweig, M.R., Bennett, E.L., Colombo, P.J., Lee, D.W., and Serrano, P.A. (1993). Short-term, intermediate-term, and long-term memories. Behav. Brain Res. *57*, 193–198. https://doi.org/10.1016/0166-4328(93)90135-D.
7. Kandel, E.R., Dudai, Y., and Mayford, M.R. (2014). The molecular and systems biology of memory. Cell *157*, 163–186. https://doi.org/10.1016/j.cell.2014.03.001.
8. Inoue, A., Sawatari, E., Hisamoto, N., Kitazono, T., Teramoto, T., Fujiwara, M., Matsumoto, K., and Ishihara, T. (2013). Forgetting in C. elegans Is Accelerated by Neuronal Communication via the TIR-1/JNK-1 Pathway. Cell Rep. *3*, 808–819. https://doi.org/10.1016/j.celrep.2013.02.019.
9. Arai, M., Kurokawa, I., Arakane, H., Kitazono, T., and Ishihara, T. (2022). Regulation of Diacylglycerol Content in Olfactory Neurons Determines Forgetting or Retrieval of Olfactory Memory in Caenorhabditis elegans. J. Neurosci. *42*, 8039–8053. https://doi.org/10.1523/JNEUROSCI.0090-22.2022.
10. Rahmani, A., McMillen, A., Allen, E., Minervini, C., and Chew, Y.L. (2024). Behavioral Tests for Associative Learning in Caenorhabditis elegans. Methods Mol. Biol. *2746*, 21–46. https://doi.org/10.1007/978-1-0716-3585-8_2.
11. Stein, G.M., and Murphy, C.T. (2014). C. elegans positive olfactory associative memory is a molecularly conserved behavioral paradigm. Neurobiol. Learn. Mem. *115*, 86–94. https://doi.org/10.1016/j.nlm.2014.07.011.
12. Nishijima, S., and Maruyama, I.N. (2017). Appetitive olfactory learning and long-term associative memory in Caenorhabditis elegans. Front. Behav. Neurosci. *11*, 80. https://doi.org/10.3389/fnbeh.2017.00080.
13. Amano, H., and Maruyama, I.N. (2011). Aversive olfactory learning and associative long-term memory in Caenorhabditis elegans. Learn. Mem. *18*, 654–665. https://doi.org/10.1101/lm.2224411.
14. Beck, C.D., and Rankin, C.H. (1995). Heat shock disrupts long-term memory consolidation in Caenorhabditis elegans. Learn. Mem. *2*, 161–177. https://doi.org/10.1101/lm.2.3-4.161.
15. Morrison, G.E., and Van Der Kooy, D. (1997). Cold shock before associative conditioning blocks memory retrieval, but cold shock after conditioning blocks memory retention in Caenorhabditis elegans. Behav. Neurosci. *111*, 564–578. https://doi.org/10.1037/0735-7044.111.3.564.
16. Kauffman, A.L., Ashraf, J.M., Corces-Zimmerman, M.R., Landis, J.N., and Murphy, C.T. (2010). Insulin signaling and dietary restriction differentially influence the decline of learning and memory with age. PLoS Biol. *8*, e1000372. https://doi.org/10.1371/journal.pbio.1000372.
17. Vukojevic, V., Gschwind, L., Vogler, C., Demougin, P., De Quervain, D.J.F., Papassotiropoulos, A., and Stetak, A. (2012). A role for α-adducin (ADD-1) in nematode and human memory. EMBO J. *31*, 1453–1466. https://doi.org/10.1038/emboj.2012.14.
18. Patel, H., and Zamani, R. (2021). The role of PKMζ in the maintenance of long-term memory: A review. Rev. Neurosci. *32*, 481–494. https://doi.org/10.1515/revneuro-2020-0105.
19. Van Damme, S., De Fruyt, N., Watteyne, J., Kenis, S., Peymen, K., Schoofs, L., and Beets, I. (2021). Neuromodulatory pathways in learning and memory: Lessons from invertebrates. J. Neuroendocrinol. *33*, e12911. https://doi.org/10.1111/jne.12911.
20. Rahmani, A., and Chew, Y.L. (2021). Investigating the Molecular Mechanisms of Learning and Memory Using Caenorhabditis

elegans (John Wiley & Sons, Ltd). https://doi.org/10.1111/jnc.15510.
21. Tabone, C.J., and De Belle, J.S. (2011). Second-order conditioning in Drosophila. Learn. Mem. *18*, 250–253. https://doi.org/10.1101/lm.2035411.
22. Lee, J.C. (2021). Second-Order Conditioning in Humans (Frontiers Media S.A.). https://doi.org/10.3389/fnbeh.2021.672628.
23. Pokala, N., Liu, Q., Gordus, A., and Bargmann, C.I. (2014). Inducible and titratable silencing of Caenorhabditis elegans neurons *in vivo* with histamine-gated chloride channels. Proc. Natl. Acad. Sci. USA *111*, 2770–2775. https://doi.org/10.1073/pnas.1400615111.
24. Liu, H., Wu, T., Canales, X.G., Wu, M., Choi, M.K., Duan, F., Calarco, J.A., and Zhang, Y. (2022). Forgetting generates a novel state that is reactivatable. Sci. Adv. *8*, 9071. https://doi.org/10.1126/sciadv.abi9071.
25. Cho, C.E., Brueggemann, C., L'Etoile, N.D., and Bargmann, C.I. (2016). Parallel encoding of sensory history and behavioral preference during Caenorhabditis elegans olfactory learning. Elife *5*, e14000. https://doi.org/10.7554/eLife.14000.
26. Freytag, V., Probst, S., Hadziselimovic, N., Boglari, C., Hauser, Y., Peter, F., Gabor Fenyves, B., Milnik, A., Demougin, P., Vukojevic, V., et al. (2017). Genome-wide temporal expression profiling in Caenorhabditis elegans identifies a core gene set related to long-term memory. J. Neurosci. *37*, 6661–6672. https://doi.org/10.1523/JNEUROSCI.3298-16.2017.
27. Lakhina, V., Arey, R.N., Kaletsky, R., Kauffman, A., Stein, G., Keyes, W., Xu, D., and Murphy, C.T. (2015). Genome-wide functional analysis of CREB/Long-term memory-dependent transcription reveals distinct basal and memory gene expression programs. Neuron *85*, 330–345. https://doi.org/10.1016/j.neuron.2014.12.029.
28. Kaletsky, R., Yao, V., Williams, A., Runnels, A.M., Tadych, A., Zhou, S., Troyanskaya, O.G., and Murphy, C.T. (2018). Transcriptome analysis of adult Caenorhabditis elegans cells reveals tissue-specific gene and isoform expression. PLoS Genet. *14*, e1007559. https://doi.org/10.1371/journal.pgen.1007559.
29. Chen, Y.-J., Wu, S.-J., Tang, Y.-C., Wu, Y.-C., Chiang, Y.-C., and Pan, C.-L. (2023). Transcriptome and Mutant Analysis of Neuronal Genes for Memory Formation and Retrieval in Caenorhabditis elegans. bioRxiv *2023*, 10. https://doi.org/10.1101/2023.10.31.564890.
30. Sternberg, P.W., Van Auken, K., Wang, Q., Wright, A., Yook, K., Zarowiecki, M., Arnaboldi, V., Becerra, A., Brown, S., Cain, S., et al. (2024). WormBase 2024: status and transitioning to Alliance infrastructure. Genetics *227*, iyae050. https://doi.org/10.1093/GENETICS/IYAE050.
31. Bateman, A., Martin, M.J., Orchard, S., Magrane, M., Ahmad, S., Alpi, E., Bowler-Barnett, E.H., Britto, R., Bye-A-Jee, H., Cukura, A., et al. (2023). UniProt: the Universal Protein Knowledgebase in 2023. Nucleic Acids Res. *51*, D523–D531. https://doi.org/10.1093/NAR/GKAC1052.
32. Michalakis, S., Kleppisch, T., Polta, S.A., Wotjak, C.T., Koch, S., Rammes, G., Matt, L., Becirovic, E., and Biel, M. (2011). Altered synaptic plasticity and behavioral abnormalities in CNGA3-deficient mice. Genes Brain Behav. *10*, 137–148. https://doi.org/10.1111/J.1601-183X.2010.00646.X.
33. Song, W., Li, Q., Wang, T., Li, Y., Fan, T., Zhang, J., Wang, Q., Pan, J., Dong, Q., Sun, Z.S., and Wang, Y. (2022). Putative complement control protein CSMD3 dysfunction impairs synaptogenesis and induces neurodevelopmental disorders. Brain Behav. Immun. *102*, 237–250. https://doi.org/10.1016/J.BBI.2022.02.027.
34. Uddin, R.K., and Singh, S.M. (2013). Hippocampal Gene Expression Meta-Analysis Identifies Aging and Age-Associated Spatial Learning Impairment (ASLI) Genes and Pathways. PLoS One *8*, e69768. https://doi.org/10.1371/JOURNAL.PONE.0069768.
35. Nozal, V., and Martinez, A. (2019). Tau Tubulin Kinase 1 (TTBK1), a new player in the fight against neurodegenerative diseases. Eur. J. Med. Chem. *161*, 39–47. https://doi.org/10.1016/J.EJMECH.2018.10.030.
36. Feng, H., Khalil, S., Neubig, R.R., and Sidiropoulos, C. (2018). A mechanistic review on GNAO1-associated movement disorder. Neurobiol. Dis. *116*, 131–141. https://doi.org/10.1016/J.NBD.2018.05.005.
37. Du, K., Lu, W., Sun, Y., Feng, J., and Wang, J.H. (2019). mRNA and miRNA profiles in the nucleus accumbens are related to fear memory and anxiety induced by physical or psychological stress. J. Psychiatr. Res. *118*, 44–65. https://doi.org/10.1016/J.JPSYCHIRES.2019.08.013.
38. De Souza Silva, M.A., Lenz, B., Rotter, A., Biermann, T., Peters, O., Ramirez, A., Jessen, F., Maier, W., Hüll, M., Schröder, J., et al. (2013). Neurokinin3 receptor as a target to predict and improve learning and memory in the aged organism. Proc. Natl. Acad. Sci. USA *110*, 15097–15102. https://doi.org/10.1073/pnas.1306884110.
39. Kanwal, A., Pardo, J.V., and Naz, S. (2022). RGS3 and IL1RAPL1 missense variants implicate defective neurotransmission in early-onset inherited schizophrenias. J. Psychiatry Neurosci. *47*, E379–E390. https://doi.org/10.1503/JPN.220070.
40. Liu, D., Dai, S.X., He, K., Li, G.H., Liu, J., Liu, L.G., Huang, J.F., Xu, L., and Li, W.X. (2021). Identification of hub ubiquitin ligase genes affecting Alzheimer's disease by analyzing transcriptome data from multiple brain regions. Sci. Prog. *104*, 368504211001146. https://doi.org/10.1177/00368504211001146.
41. Natunen, T., Martiskainen, H., Sarajärvi, T., Helisalmi, S., Pursiheimo, J.P., Viswanathan, J., Laitinen, M., Mäkinen, P., Kauppinen, T., Rauramaa, T., et al. (2013). Effects of NR1H3 Genetic Variation on the Expression of Liver X Receptor α and the Progression of Alzheimer's Disease. PLoS One *8*, e80700. https://doi.org/10.1371/JOURNAL.PONE.0080700.
42. Held, K., and Tóth, B.I. (2021). TRPM3 in Brain (Patho)Physiology. Front. Cell Dev. Biol. *9*, 635659. https://doi.org/10.3389/fcell.2021.635659.
43. Song, Y.H., Yoon, J., and Lee, S.H. (2021). The role of neuropeptide somatostatin in the brain and its application in treating neurological disorders. Exp. Mol. Med. *53*, 328–338. https://doi.org/10.1038/s12276-021-00580-4.
44. De Filippis, B., Lyon, L., Taylor, A., Lane, T., Burnet, P.W.J., Harrison, P.J., and Bannerman, D.M. (2015). The role of group II metabotropic glutamate receptors in cognition and anxiety: Comparative studies in GRM2−/−, GRM3−/− and GRM2/3−/− knockout mice. Neuropharmacology *89*, 19–32. https://doi.org/10.1016/J.NEUROPHARM.2014.08.010.
45. Bishop, J.R., Reilly, J.L., Harris, M.S.H., Patel, S.R., Kittles, R., Badner, J.A., Prasad, K.M., Nimgaonkar, V.L., Keshavan, M.S., and Sweeney, J.A. (2015). Pharmacogenetic associations of the type-3 metabotropic glutamate receptor (GRM3) gene with working memory and clinical symptom response to antipsychotics in first-episode schizophrenia. Psychopharmacology (Berl) *232*, 145–154. https://doi.org/10.1007/S00213-014-3649-4/METRICS.
46. Dubos, A., Meziane, H., Iacono, G., Curie, A., Riet, F., Martin, C., Loaëc, N., Birling, M.C., Selloum, M., Normand, E., et al. (2018). A new mouse model of ARX dup24 recapitulates the patients' behavioral and fine motor alterations. Hum. Mol. Genet. *27*, 2138–2153. https://doi.org/10.1093/HMG/DDY122.
47. Song, T., Liang, S., Liu, J., Zhang, T., Yin, Y., Geng, C., Gao, S., Feng, Y., Xu, H., Guo, D., et al. (2018). CRL4 antagonizes SCFFbxo7-mediated turnover of cereblon and BK channel to regulate learning and memory. PLoS Genet. *14*, e1007165. https://doi.org/10.1371/JOURNAL.PGEN.1007165.
48. Chu, L.-A., Lu, C.-H., Yang, S.-M., Feng, K.-L., Liu, Y.-T., Chen, C.-C., Tsai, Y.-C., Chen, P., Lee, T.-K., Hwu, Y.-K., et al. (2018). Visualization of axonal protein allocation in Drosophila with whole-brain localization microscopy. bioRxiv *2018*, 454942. https://doi.org/10.1101/454942.
49. Pilorge, M., Fassier, C., Le Corronc, H., Potey, A., Bai, J., De Gois, S., Delaby, E., Assouline, B., Guinchat, V., Devillard, F., et al. (2015). Genetic and functional analyses demonstrate a role for abnormal glycinergic signaling in autism. Mol. Psychiatry *21*, 936–945. https://doi.org/10.1038/mp.2015.139.
50. Cai, H.Y., Chen, S.R., Wang, Y., Jiao, J.J., Qiao, J., Hölscher, C., Wang, Z.J., Zhang, S.X., and Wu, M.N. (2023). Integrated analysis of the lncRNA-associated ceRNA network in Alzheimer's disease. Gene *876*, 147484. https://doi.org/10.1016/J.GENE.2023.147484.
51. Kida, S. (2019). Reconsolidation/destabilization, extinction and forgetting of fear memory as therapeutic targets for PTSD. Psychopharmacology (Berl) *236*, 49–57. https://doi.org/10.1007/S00213-018-5086-2.
52. Torayama, I., Ishihara, T., and Katsura, I. (2007). Caenorhabditis elegans Integrates the Signals of Butanone and Food to Enhance Chemotaxis to Butanone. J. Neurosci. *27*, 741–750. https://doi.org/10.1523/JNEUROSCI.4312-06.2007.
53. Liao, C.P., Chiang, Y.C., Tam, W.H., Chen, Y.J., Chou, S.H., and Pan, C.L. (2022). Neurophysiological basis of stress-induced aversive memory in the nematode Caenorhabditis elegans. Curr. Biol. *32*, 5309–5322.e6. https://doi.org/10.1016/J.CUB.2022.11.012.
54. Zhang, Y., Lu, H., and Bargmann, C.I. (2005). Pathogenic bacteria induce aversive olfactory learning in Caenorhabditis elegans. Nature *438*, 179–184. https://doi.org/10.1038/nature04216.
55. Wong, J.S.H., and Rankin, C.H. (2019). Caenorhabditis elegans Learning and Memory. In Oxford Research Encyclopedia of Neuroscience. https://doi.org/10.1093/ACREFORE/9780190264086.013.282.
56. Pritz, C., Itskovits, E., Bokman, E., Ruach, R., Gritsenko, V., Nelken, T., Menasherof, M.,

Azulay, A., and Zaslaver, A. (2023). Principles for coding associative memories in a compact neural network. Elife *12*, e74434. https://doi.org/10.7554/ELIFE.74434.

57. Ghirardi, M., Montarolo, P.G., and Kandel, E.R. (1995). A novel intermediate stage in the transition between short- and long-term facilitation in the sensory to motor neuron synapse of aplysia. Neuron *14*, 413–420. https://doi.org/10.1016/0896-6273(95)90297-X.
58. Sutton, M.A., and Carew, T.J. (2002). Behavioral, Cellular, and Molecular Analysis of Memory in Aplysia I: Intermediate-Term Memory. In Integrative and Comparative Biology (Oxford Academic), pp. 725–735. https://doi.org/10.1093/icb/42.4.725.
59. Walz, R., Roesler, R., Quevedo, J., Sant'Anna, M.K., Madruga, M., Rodrigues, C., Gottfried, C., Medina, J.H., and Izquierdo, I. (2000). Time-dependent impairment of inhibitory avoidance retention in rats by posttraining infusion of a mitogen-activated protein kinase kinase inhibitor into cortical and limbic structures. Neurobiol. Learn. Mem. *73*, 11–20. https://doi.org/10.1006/nlme.1999.3913.
60. Igaz, L.M., Vianna, M.R.M., Medina, J.H., and Izquierdo, I. (2002). Two Time Periods of Hippocampal mRNA Synthesis Are Required for Memory Consolidation of Fear-Motivated Learning. J. Neurosci. *22*, 6781–6789. https://doi.org/10.1523/JNEUROSCI.22-15-06781.2002.
61. Shrestha, P., Ayata, P., Herrero-Vidal, P., Longo, F., Gastone, A., LeDoux, J.E., Heintz, N., and Klann, E. (2020). Cell-type-specific drug-inducible protein synthesis inhibition demonstrates that memory consolidation requires rapid neuronal translation. Nat. Neurosci. *23*, 281–292. https://doi.org/10.1038/s41593-019-0568-z.
62. Tintorelli, R., Budriesi, P., Villar, M.E., Marchal, P., Lopes da Cunha, P., Correa, J., Giurfa, M., and Viola, H. (2020). Spatial-Memory Formation After Spaced Learning Involves ERKs1/2 Activation Through a Behavioral-Tagging Process. Sci. Rep. *10*, 98. https://doi.org/10.1038/s41598-019-57007-4.
63. MacCallum, P.E., and Blundell, J. (2020). The mTORC1 inhibitor rapamycin and the mTORC1/2 inhibitor AZD2014 impair the consolidation and persistence of contextual fear memory. Psychopharmacology (Berl) *237*, 2795–2808. https://doi.org/10.1007/S00213-020-05573-1.
64. Mac Callum, P.E., Hebert, M., Adamec, R.E., and Blundell, J. (2014). Systemic inhibition of mTOR kinase via rapamycin disrupts consolidation and reconsolidation of auditory fear memory. Neurobiol. Learn. Mem. *112*, 176–185. https://doi.org/10.1016/J.NLM.2013.08.014.
65. Restivo, L., Vetere, G., Bontempi, B., and Ammassari-Teule, M. (2009). The formation of recent and remote memory is associated with time-dependent formation of dendritic spines in the hippocampus and anterior cingulate cortex. J. Neurosci. *29*, 8206–8214. https://doi.org/10.1523/JNEUROSCI.0966-09.2009.
66. Dudai, Y., Karni, A., and Born, J. (2015). The Consolidation and Transformation of Memory. Neuron *88*, 20–32. https://doi.org/10.1016/J.NEURON.2015.09.004.
67. Prahlad, V., Cornelius, T., and Morimoto, R.I. (2008). Regulation of the cellular heat shock response in Caenorhabditis elegans by thermosensory neurons. Science *320*, 811–814. https://doi.org/10.1126/science.1156093.
68. Zhou, S., Zhang, Y., Kaletsky, R., Toraason, E., Zhang, W., Dong, M.-Q., and Murphy, C.T. (2023). Signaling from the C. elegans Hypodermis Non-autonomously Facilitates Short-term Associative Memory. Preprint at bioRxiv. https://doi.org/10.1101/2023.02.16.528821.
69. Belgacem, Y.H., and Borodinsky, L.N. (2017). CREB at the crossroads of activity-dependent regulation of nervous system development and function. In Advances in Experimental Medicine and Biology, pp. 19–39. https://doi.org/10.1007/978-3-319-62817-2_2.
70. Templeman, N.M., Cota, V., Keyes, W., Kaletsky, R., and Murphy, C.T. (2020). CREB Non-autonomously Controls Reproductive Aging through Hedgehog/Patched Signaling. Dev. Cell *54*, 92–105.e5. https://doi.org/10.1016/j.devcel.2020.05.023.
71. Hegde, A.N. (2017). Proteolysis, synaptic plasticity and memory. Neurobiol. Learn. Mem. *138*, 98–110. https://doi.org/10.1016/J.NLM.2016.09.003.
72. Kudryashova, I.V. (2009). Proteolysis and proteolytic enzymes in structural plasticity of synapses. Neurochem. J. *3*, 164–172. https://doi.org/10.1134/S1819712409030027/METRICS.
73. Nguyen, K.M., and Busino, L. (2020). The Biology of F-box Proteins: The SCF Family of E3 Ubiquitin Ligases. Adv. Exp. Med. Biol. *1217*, 111–122. https://doi.org/10.1007/978-981-15-1025-0_8/TABLES/1.
74. Tischmeyer, W., and Grimm, R. (1999). Activation of immediate early genes and memory formation. Cell. Mol. Life Sci. *55*, 564–574. https://doi.org/10.1007/S000180050315/METRICS.
75. Wang, Y., Luo, W., and Reiser, G. (2008). Trypsin and trypsin-like proteases in the brain: Proteolysis and cellular functions. Cell. Mol. Life Sci. *65*, 237–252. https://doi.org/10.1007/S00018-007-7288-3/METRICS.
76. Hukema, R.K., Rademakers, S., and Jansen, G. (2008). Gustatory plasticity in C. elegans involves integration of negative cues and NaCl taste mediated by serotonin, dopamine, and glutamate. Learn. Mem. *15*, 829–836. https://doi.org/10.1101/LM.994408.
77. Colbert, H.A., and Bargmann, C.I. (1997). Environmental signals modulate olfactory acuity, discrimination, and memory in Caenorhabditis elegans. Learn. Mem. *4*, 179–191. https://doi.org/10.1101/LM.4.2.179.
78. Kindt, K.S., Quast, K.B., Giles, A.C., De, S., Hendrey, D., Nicastro, I., Rankin, C.H., and Schafer, W.R. (2007). Dopamine Mediates Context-Dependent Modulation of Sensory Plasticity in C. elegans. Neuron *55*, 662–676. https://doi.org/10.1016/j.neuron.2007.07.023.
79. Chen, S., Zhou, Y., Chen, Y., and Gu, J. (2018). fastp: an ultra-fast all-in-one FASTQ preprocessor. Bioinformatics *34*, i884. https://doi.org/10.1101/274100.
80. Kim, D., Langmead, B., and Salzberg, S.L. (2015). HISAT: a fast spliced aligner with low memory requirements. Nat. Methods *12*, 357–360. https://doi.org/10.1038/nmeth.3317.
81. Liao, Y., Smyth, G.K., and Shi, W. (2014). featureCounts: an efficient general purpose program for assigning sequence reads to genomic features. Bioinformatics *30*, 923–930. https://doi.org/10.1093/BIOINFORMATICS/BTT656.
82. Love, M.I., Huber, W., and Anders, S. (2014). Moderated estimation of fold change and dispersion for RNA-seq data with DESeq2. Genome Biol. *15*, 550. https://doi.org/10.1186/S13059-014-0550-8/FIGURES/9.
83. Robinson, M.D., McCarthy, D.J., and Smyth, G.K. (2010). edgeR: a Bioconductor package for differential expression analysis of digital gene expression data. Bioinformatics *26*, 139–140. https://doi.org/10.1093/BIOINFORMATICS/BTP616.
84. Zhang, Y., Parmigiani, G., and Johnson, W.E. (2020). ComBat-seq: batch effect adjustment for RNA-seq count data. NAR Genom. Bioinform. *2*, lqaa078. https://doi.org/10.1093/NARGAB/LQAA078.
85. Hulsen, T., de Vlieg, J., and Alkema, W. (2008). BioVenn - A web application for the comparison and visualization of biological lists using area-proportional Venn diagrams. BMC Genom. *9*, 488. https://doi.org/10.1186/1471-2164-9-488.
86. Gu, Z., Eils, R., and Schlesner, M. (2016). Complex heatmaps reveal patterns and correlations in multidimensional genomic data. Bioinformatics *32*, 2847–2849. https://doi.org/10.1093/BIOINFORMATICS/BTW313.
87. Afgan, E., Nekrutenko, A., Grüning, B.A., Blankenberg, D., Goecks, J., Schatz, M.C., Ostrovsky, A.E., Mahmoud, A., Lonie, A.J., Syme, A., et al. (2022). The Galaxy platform for accessible, reproducible and collaborative biomedical analyses: 2022 update. Nucleic Acids Res. *50*, W345–W351. https://doi.org/10.1093/NAR/GKAC247.
88. Holdorf, A.D., Higgins, D.P., Hart, A.C., Boag, P.R., Pazour, G.J., Walhout, A.J.M., and Walker, A.K. (2020). WormCat: An Online Tool for Annotation and Visualization of Caenorhabditis elegans Genome-Scale Data. Genetics *214*, 279–294. https://doi.org/10.1534/GENETICS.119.302919.

STAR★METHODS

KEY RESOURCES TABLE

REAGENT or RESOURCE	SOURCE	IDENTIFIER
Bacterial and virus strains		
Escherichia coli OP50	CGC	RRID:WB-STRAIN:WBStrain00041969
Chemicals, peptides, and recombinant proteins		
Hydrochloric acid solution	Sigma-Aldrich	Cat# H9892
Diacetyl	Sigma-Aldrich	Cat# B85307
Isoamyl alcohol	Sigma-Aldrich	Cat# 320021
Cycloheximide	Sigma-Aldrich	Cat# 01810
Actinomycin D	Sigma-Aldrich	Cat# A4262
Histamine dihydrochloride	Sigma-Aldrich	Cat# H7250
TRI Reagent	Sigma-Aldrich	Cat# T3934
Fast SYBR™ Green Master Mix	Thermo Fisher	Cat# 4385612
Critical commercial assays		
High-Capacity cDNA Reverse Transcription Kit	Thermo Fisher	Cat# 4368814
NucleoSpin RNA, Mini kit for RNA purification	MACHEREY-NAGEL	Cat# 740955.50
KAPA Stranded mRNA-Seq Kit, with KAPA mRNA Capture Beads	Kapa Biosystems	Cat# KK8420
Deposited data		
Raw RNA-seq data	this paper	PRJNA: 1113216
Experimental models: organisms/strains		
C. elegans N2	Caenorhabditis elegans Genetic Center	RRID:WB-STRAIN:WBStrain00000001
C. elegans IRB4000 *yesIs1[Psra-6::HisCl1:: SL2::mCherry + Pelt-2::mCherry]*	this manuscript	N/A
C. elegans IRB4001 *yesIs2[odr-10p::HisCl1; unc-122p::gfp]*	this manuscript	N/A
See Table 1 for a list of all *C. elegans* mutant strains	Caenorhabditis elegans Genetic Center	N/A
Oligonucleotides		
See Table S10 for a list of oligonucleotides	IDT Integrated DNA Technologies	N/A
Software and algorithms		
Prism 10	Graphpad	
FASTQ	Chen et al.[79]	
HISAT2	Kim et al.[80]	
featureCounts	Liao et al.[81]	
DESeq2	Love et al.[82]	version 1.42.1
edgeR	Robinson et al.[83]	version 3.43.7
Combat-Seq	Zhang et al.[84]	version 3.49.0
BioVenn	Hulsen et al.[85]	
ComplexHeatmap	Gu et al.[86]	

EXPERIMENTAL MODEL AND STUDY PARTICIPANT DETAILS

Caenorhabditis elegans

C. elegans were cultured on nematode growth medium (NGM) agar plates produced by Hylabs (Rehovot, Israel), consistently maintained at 22°C. Synchronization of worms was achieved by bleaching gravid hermaphrodites to extract fertile eggs, which were then transferred onto NGM plates pre-seeded with OP50 bacteria. All worms used in this study were synchronized and kept in well-fed conditions on standard NGM

plates for three days prior to experimentation. Drugs and chemicals used as stimuli were diluted in double distilled water (DDW). All experiments were conducted at room temperature (22°C-24°C).

Unless otherwise mentioned, the reference control strain in each experiment was the N2 Bristol strain. To generate integrated strains, IRB4001 and IRB4000, carrying histamine-gated chloride (HisCl) channels in AWA and ASH neurons, respectively, we exposed strains ZC3160 and CX15206, kind gifts from Yun Zhang and Cornelia I. Bargmann, carrying the HisCl transgene on extrachromosomal arrays *yxEx1638[Podr-10::HisCl1, Punc-122p::GFP]* and *kyEx5104[Psra-6::HisCl1::SL2::mCherry, Pelt-2::mCherry]*, respectively, to 400 J/cm^2 UV irradiation using a UVC-508 ultraviolet crosslinker. The exposure was done in small 6 cm bacteria-free NGM plate with the lid removed. Following irradiation, worms were kept overnight in 15°C. We then selected and isolated integrated lines. These were outcrossed 6 times with N2. Additional mutant strains used in this study are listed in Table 2.

METHOD DETAILS

Behavioral assays

Detailed parameters for each behavioral experiment are provided in Table S2.

Aversive conditioning

Synchronized adult worms were gently rinsed off their growth plates using double distilled water (DDW) and transferred into standard Eppendorf tubes with a glass pipette. After a 1 min settling period, the supernatant was carefully removed, and replaced by 700 μL DDW. This washing process was repeated 5–6 times to ensure thorough removal of any residual bacteria. In the final wash M9 buffer was used instead of DDW. Subsequently, the worms were subjected to a 2 h starvation period by placing them on fresh bacteria-free NGM plates.[11,76,77] Following starvation, the worms were collected into new Eppendorf tubes, and excess supernatant was gently removed.

In each tube, 250 μL of the conditioning or control solution was added. The conditioning solutions comprised Diacetyl (Sigma Aldrich B85307) in a 1:10,000 dilution, 1 mM (pH = 3) HCl (Sigma Aldrich H9892), or a combination of both (unless otherwise specified in the figure legend or Table S2). The worms were then incubated with the conditioning solution for a total of 15 min. Throughout this period, the tubes were positioned on their side on an isolated shelf to minimize environmental disturbances and facilitate worm dispersion within the tube. Approximately 30 s before the conclusion of the 15 min training period, the tubes were returned to their upright position, allowing the worms approximately 25 s to settle. Following the 15 min conditioning period, the conditioning solution was carefully aspirated, and the worms were rinsed once with 700 μL of DDW. After the rinse, the tubes where centrifuge for 1–2 s in mini centrifuge at 6,000 RPM, and the supernatant was removed.

For adaptation experiments, worms underwent the same procedure as for aversive conditioning, omitting, however, the initial starvation step.

Chemotaxis testing was performed immediately after rinsing the worms. However, when testing memory at later time points, and up to 4 h post conditioning, worms were incubated in 250 μL DDW in the interim between conditioning and testing. When testing for memory retention 18 h post conditioning, worms were transferred to fresh NGM plates pre-seeded with OP50 bacteria, and incubated at 15°C, after which worms were collected from the plates and washed three times with 700 μL DDW before proceeding to the chemotaxis assay.

Chemotaxis assay

To test chemotaxis, we first allowed fresh bacteria-free NGM 85 mm test plates to dry without lids for 1 h. We then spotted one end of the plate (Figure S7) with 3 μL diacetyl at a dilution of 1:1,000 (unless otherwise mentioned in the figure legends or in Table S2). 10 min prior to the start of the chemotaxis experiment, 1 μL of 1M sodium azide was added to the diacetyl spot for worm immobilization. Approximately 200 worms were transferred to the center of the plate using a glass pipette. The worms were gently dried with a Kimwipe, the lids of the plates were closed, and the worms were allowed to move freely for 15 min (unless indicated otherwise). To conclude the experiment, the test plates were subjected to a few seconds of heat in a microwave oven to halt worm movement. Subsequently, the number of worms on the odor side (A) of the plate and an equivalent region (B) on the other side of the plate were counted (Figure S7). Worms within the start point region (Figure S7) were excluded from the count. The chemotaxis index was calculated using the formula: Chemotaxis Index = (#Side A - #Side B)/(#Side A + #Side B). The learning or memory index was determined as follows: Learning Index or Memory Index = (#Control Worms - #Conditioned Worms)/#Control Worms.

Second order conditioning

The second-order conditioning protocol was similar to the aversive conditioning protocol with several adjustments. First, the pre-conditioning starvation period was only 1 h long. Second, during conditioning, worms underwent two consecutive 10 min incubations with the specified chemicals, separated by a single wash with 700 μL of DDW. Finally, for the chemotaxis assay, 1:10 Isoamyl alcohol (IAA) diluted in ethanol was utilized as chemoattractant.

Blocking neuronal activity, transcription and translation

To examine the requirement and timing of neuronal activity as well as transcription and translation, we applied a pulse treatment of 250 μL 10 mM histamine dihydrochloride (Sigma Aldrich H7250), 0.8 mg/mL Cycloheximide (Sigma Aldrich 01810), or 50 μg/mL Actinomycin D

(Sigma Aldrich A4262) diluted in DDW, to the Eppendorf tube for 5 min at specific time points after conditioning. Subsequently, a single wash with 700 μL of DDW was performed, followed by continued incubation in DDW until the chemotaxis assay was conducted.

Naive chemotaxis with or without histamine treatment

To test the direct effects of histamine treatment (Figures 3A–3C) on chemotaxis, synchronized adult worms were gently washed off their growth plates using DDW and transferred to standard Eppendorf tubes using a glass pipette. After a 1 min settling period, the supernatant was removed, and this washing procedure was repeated 3 times with 700 μL DDW to ensure the removal of any residual bacteria. Finally, the supernatant was carefully removed, and worms were incubated with 10 mM histamine for 3 min, followed by a 15 min chemotaxis assay.

Transcriptional profiling

RNA extraction and sequencing

RNA extraction was performed following conditioning and incubation for 20, 40 or 60 min. The DDW supernatant was removed from each sample, and 300 μL of TRIzol was added to an approximate volume of 100 μL of adult worms. Subsequently, the sample was flash-frozen in liquid nitrogen. Once all samples had been frozen, they were subjected to 10 rapid freeze-thaw cycles in liquid nitrogen, until only intact eggs could be observed in the solution.

RNA purification was performed using the NucleoSpin RNA kit (Macherey-Nagel, Duren Germany #740955.50). Lysis was done using 10 rapid freeze-thaw cycles. Therefore, we started form step 3 of the protocol (Filtrate lysate). RNA quality was assessed using Agilent 2200 TapeStation analysis. For mRNA library preparation, the KAPA Stranded mRNA-Seq Kit with mRNA Capture Beads (Kapa Biosystems, KK8420) was utilized. In brief, 1 μg of RNA was used for library construction following the manufacturer's recommendations, and the library was eluted in 20 μL of elution buffer. Libraries were then adjusted to 10 mM and loaded onto the Novaseq 6000 machine (Illumina) for sequencing, generating an average of 35 million reads per sample with 122 bp single-end reads. The raw RNA-seq data can be found at the National Center for Biotechnology Information Sequence Read Archive: https://www.ncbi.nlm.nih.gov/sra/PRJNA1113216.

RNA-seq analysis

For RNA-seq analysis, Fastq files were uploaded to the Galaxy project web platform, and the public server at usegalaxy.org [87] was used to analyze the data. Quality control steps including low-quality reads filtering, trimming of low-quality bases, and adapter detection and trimming were performed using FASTQ[79] with default settings. Subsequently, reads were aligned to the WBcel235 reference genome using HISAT2.[80] Gene expression quantification was conducted using featureCounts.[81]

Normalization of library sizes and principal component analysis (PCA) were carried out using the DESeq2 R package (version 1.42.1).[82] Genes with a sum count of less than 12 across all samples were filtered out. Differential expression analysis for each time point was performed using the Bioconductor edgeR package (version 3.43.7)[83] in R, following batch-effect correction with the Combat-Seq R package (version 3.49.0).[84] Genes were deemed significantly differentially expressed if they exhibited a fold change of at least 15% with a p value smaller than 0.05. Venn diagrams were plotted using BioVenn.[85]

Hierarchical clustering and heatmap

For Hierarchical clustering and Heatmap analysis, a total of 1,381 detected DEGs were utilized to provide a comprehensive overview of gene expression levels across time points following conditioning. All samples were categorized into four groups: the control group, comprising the average of all control samples across all time points, and the remaining groups, each containing the average of conditioning samples for each respective time point. Values were Z score normalized, and a heatmap was generated using the ComplexHeatmap R package in R Studio.[86] Euclidean distance and average linkage clustering methods were employed to construct a hierarchical clustering analysis on the rows. The rows were then divided into four clusters, and for each cluster, values were normalized as percentages relative to the control column values. Subsequently, the data were plotted using Graphpad Prism 10.

Gene ontology analysis via WormCat

Gene ontology (GO) enrichment analysis was conducted using WormCat,[88] a *C. elegans*-specific tool for GO enrichment analysis and visualization (available at http://wormcat.com/). A total of 1,381 significantly up- or downregulated genes were input into WormCat using default settings. Terms were considered statistically enriched when the reported p values were less than 0.05, determined by Fisher's exact test. The UNASSIGNED gene category was excluded from the analysis. To compare between GO terms in our current DEG dataset and previous datasets,[26,27] we searched for Category 3 GO terms, significantly enriched in all 3 datasets.

Reverse transcription quantitative PCR (RT-qPCR)

RNA extraction and purification were conducted as for Transcriptional profiling (see above). cDNA was produced by reverse transcription of RNA samples with a High-Capacity cDNA Reverse Transcription kit (Applied Biosystems, CA; #4368814).

qPCR was performed in duplicates using the Fast SYBR Green Master Mix (Applied Biosystems; #4385612) and quantified in a QS5 Real-Time PCR (96 wells) detection system (Applied Biosystems). Relative mRNA expression was calculated using the DDCT method relative to K07A1.10 as a reference gene. Primer sequences can be found in Table S11.

Mutant memory-related homolog analysis

Gene homologs related to the subset of mutant strains that we tested (Table 3) were identified using the "Homology" section of the gene report pages on WormBase (www.wormbase.org). For each homolog a literature search using Google Scholar (https://scholar.google.com) was performed with the search term: [gene name] AND memory.

QUANTIFICATION AND STATISTICAL ANALYSIS

All behavioral data were analyzed using Graphpad Prism 10. Key results are shown in the figures. Raw data together with detailed descriptions of the statistical tests and their results are provided as source data files. These can be viewed using a licensed or free of charge view mode only Prism version available at https://www.graphpad.com/updates.